

## Research paper

# AKAP2-anchored extracellular signal-regulated kinase 1 (ERK1) regulates cardiac myofibroblast migration

Marion Delaunay, Aleksandra Paterek, Ivan Gautschi, Greta Scherler, Dario Diviani\*

Department of Biomedical Sciences, Faculty of Biology et Medicine, University of Lausanne, 1011 Lausanne, Switzerland



## ARTICLE INFO

## Keywords:

A kinase anchoring protein (AKAP)  
Kinases  
Cardiac fibrosis  
Cardiac remodeling  
Cell migration

## ABSTRACT

Cardiac fibrosis is a major cause of dysfunctions and arrhythmias in failing hearts. At the cellular level fibrosis is mediated by cardiac myofibroblasts, which display an increased migratory capacity and secrete large amounts of extracellular matrix. These properties allow myofibroblasts to invade, remodel and stiffen the myocardium and eventually alter cardiac function. While the enhanced ability of cardiac myofibroblasts to migrate has been proposed to contribute to the initiation of the fibrotic process, the molecular mechanisms controlling their motile function have been poorly defined. In this context, our current findings indicate that A-kinase anchoring protein 2 (AKAP2) associates with actin at the leading edge of migrating cardiac myofibroblasts. Proteomic analysis of the AKAP2 interactome revealed that this anchoring protein assembles a signaling complex composed of the extracellular regulated kinase 1 (ERK1) and its upstream activator Grb2 that mediates the activation of ERK in cardiac myofibroblasts. Silencing AKAP2 expression results in a significant reduction in the phosphorylation of ERK1 and its downstream effector WAVE2, a protein involved in actin polymerization, and impairs the ability of cardiac myofibroblasts to migrate. Importantly, disruption of the interaction between AKAP2 and F-actin using cell-permeant competitor peptides, inhibits the activation of the ERK-WAVE2 signaling axis, resulting in a reduction of the translocation of Arp2 to the leading-edge membrane and in inhibition of cardiac myofibroblast migration. Collectively, these findings suggest that AKAP2 functions as an F-actin bound molecular scaffold mediating the activation of an ERK1-dependent promigratory transduction pathway in cardiac myofibroblasts.

## 1. Introduction

Heart failure is a pathological heart condition that leads to the progressive deterioration of cardiac function [1,2] and eventually death. The pathophysiological events that promote heart failure can be triggered by diverse cardiac insults and stresses, such as myocardial infarction (MI) and long-term hypertension [2–5]. In the long-term cardiac stress causes functional decompensation mainly as a consequence of an increased rate of cardiomyocyte apoptosis and the induction of extensive cardiac fibrosis, which profoundly impairs cardiac function [6,7]. Fibrosis increases myocardium stiffness, which promotes diastolic dysfunctions, and reduces electrical connectivity between cardiomyocytes, which increases the occurrence of life-threatening arrhythmic events [7]. In a healthy heart, fibroblasts maintain structural integrity of the myocardium by ensuring a homeostatic balance between extracellular matrix (ECM) synthesis, deposition and degradation [8]. However, in response to cardiac stress or injury, quiescent cardiac fibroblasts transdifferentiate into activated myofibroblasts,

which express the selective marker  $\alpha$ -smooth muscle actin ( $\alpha$ -SMA), are highly migratory and invasive, and secrete large amounts of ECM proteins in the intercellular space [9–11]. These properties allow cardiac myofibroblasts to invade, colonize, remodel and stiffen the stressed myocardium. Although the importance of myofibroblast migration in the pathogenesis of cardiac fibrosis is well-defined, the molecular processes involved in myofibroblast motility remain poorly understood.

The capacity of cells to sustain migration depends on continuous turnover and rearrangement of the actin cytoskeleton [12]. At the front of the cell, the extension of sheet-like actin based- structures, namely the lamellipodia, is driven by actin polymerization [13]. These structures, which lack intracellular organelles, consist of a dense actin network and provide the driving force for migration [13]. Directional cell movement is the consequence of the polymerization of branched actin filaments at lamellipodia, combined with the retraction of the rear of the cell [14]. Actin branching is mediated by Scar/WAVE that promotes actin nucleation through the association and activation of the Arp2/3 complex [15]. Scar/WAVE is included in a large regulatory complex that serves as

\* Corresponding author at: Department of Biomedical Sciences, Rue du Bugnon 27, 1011 Lausanne, Switzerland.

E-mail address: [Dario.diviani@unil.ch](mailto:Dario.diviani@unil.ch) (D. Diviani).

<https://doi.org/10.1016/j.bbamcr.2024.119674>

Received 18 September 2023; Received in revised form 22 December 2023; Accepted 10 January 2024

Available online 18 January 2024

0167-4889/© 2024 The Authors. Published by Elsevier B.V. This is an open access article under the CC BY license (<http://creativecommons.org/licenses/by/4.0/>).

integrator of multiple signaling cues controlling actin polymerization at the leading edge. Upstream activators of Scar/WAVE include the small molecular weight GTPase Rac1, phospholipids, regulatory and scaffold proteins, and kinases [15]. Over the years, phosphorylation has emerged as a central mechanism regulating Scar/WAVE activity, and multiple kinases have been shown to directly phosphorylate various components of the Scar/WAVE complex [16]. In this context, phosphorylation of the WAVE2 by a pool of extracellular signal regulated kinase (ERK) located at the leading edge of migrating cells promotes the interaction between WAVE2 and Arp2/3 [17], favors Arp2/3-mediated actin polymerization, and induces lamellipodia assembly and migration [18].

Increasing evidence suggests that the intracellular signaling events leading to cardiac fibrosis are regulated by scaffolding and anchoring proteins that compartmentalize signaling enzymes at precise cellular nanocompartments [19,20]. In this respect, a family of signal-organizing molecules, named A-kinase anchoring proteins (AKAPs), favors spatio-temporal regulation of transduction pathways by coordinating the activity of a multitude of signaling enzymes, including the cyclic adenosine monophosphate (cAMP)-dependent protein kinase (PKA), other kinases, phosphatases, and other signaling regulators [21,22]. While AKAPs have been shown to contribute to the activation of various profibrotic responses that influence cardiac myofibroblast differentiation and migration [23], the precise molecular mechanisms specifying these functions remain ill defined.

Our current study indicates that AKAP2, an anchoring protein that binds F-actin, localizes in lamellipodia of cardiac myofibroblasts. AKAP2 forms a signaling complex with Grb2 and ERK1 and promotes the phosphorylation of WAVE2 and the recruitment of the Arp2/3 complex at the leading edge of cardiac myofibroblasts, thus promoting migration. These findings suggest that AKAP2 acts as local facilitator of ERK-dependent actin remodeling and cardiac myofibroblast motility.

## 2. Material and methods

### 2.1. Plasmids and constructs

Double-stranded short hairpin (sh) oligonucleotides based upon rat AKAP2 (NCBI reference number: NM\_001011974.2: 196-2808) mRNA sequence was initially cloned into the *Hind*III and *Bgl*II sites in a pSUPER vector. The following oligonucleotide sequences were used: rat AKAP2 shRNA-1 (sense strand) 5'-GGTAGAACCCATTGAGAAA-3'; rat AKAP2 shRNA-2 (sense strand)-5'-GTACTTCAGCAAATACTCA-3' scrambled rat AKAP2 shRNA (sense strand) 5'-GCTAGATTAACGCAGAAGA-3'. To generate lentiviral transfer vectors encoding AKAP2, cDNA fragments containing the H1 RNA polymerase III promoter as well as the sequences encoding shRNAs were excised using *Eco*RI/*Kpn*I from the pSUPER vector and subcloned into the pSD28-GFP transfer vectors. pCMVDR8.91 and pMD2.VSVG helper vectors were previously described [24]. The pSD28 plasmid contains a GFP reporter gene under the control of a CMV promoter and was used to specifically target AKAP2 in neonatal rat myofibroblasts. The pFlag-ERK1 R84S construct was generated by PCR-based site directed mutagenesis using the pFlag-ERK1 plasmid as template.

### 2.2. Animal procedures

All animal experiments were performed according to the guideline for care and use of laboratory animals and approved by the Swiss Government Veterinary Office (authorization VD3680 and VD3681). The myocardial infarction was induced in the animals (C57BL/6 N) via permanent surgical ligation of the left coronary artery as previously described [25]. Briefly, mice were anesthetized by intra-peritoneal injection of ketamine/xylazine/acepromazine mixture (65/15/2 mg/kg) then intubated and placed on mechanical ventilation with a mini-rodent ventilator (tidal volume = 0.2 ml; rate = 120 breaths/min). The left coronary artery was identified and permanently ligated just below the

left atrium and for the animals undergoing a sham operation, the ligature was placed at the same location but not tied. Two weeks after surgery the animals were euthanized by overdose of anesthetic (pentobarbital solution at 50 mg/ml, 150 mg/kg intraperitoneal injection).

### 2.3. Immunohistochemistry

After sacrifice, hearts were collected and perfused ex-vivo with ice cold HBSS. Hearts were fixed in 10 % Neutral Buffered Formalin (NBF) (Merk, catalog n° HT501128) for 24 h at room temperature and subsequently included in paraffin. Paraffin blocks were cut in transversal sections of 3 µm and stained with Masson's trichrome or immunostained with the following antibodies: rabbit anti-AKAP2 (custom made, Covance, San Diego, CA, USA) or mouse monoclonal anti-AKAP2 (custom made, Absolute Antibody, United Kingdom), anti-vimentin (Sigma, mouse, ref. n° V2258), anti-alpha-smooth muscle actin (α-SMA) (Sigma, mouse, ref. n° 5228) and anti-laminin (Sigma, mouse, ref. n° L9393). Images were acquired with a Zeiss AxioScan Z.1 slide scanner with a 20× objective and with a Zeiss LSM 900 confocal microscope with a Plan-Apochromat 40×/1.30 NA oil immersion objective.

### 2.4. Isolation of cardiac myofibroblasts from neonatal rats

Rat neonatal ventricular fibroblasts (NVFs) were extracted from 2 to 3 days old Sprague Dawley rats. The hearts were excised, cut in small pieces and digested by three cycles of enzymatic digestion at 37 °C, 11000 rpm for 15 min each. For approximately 20 hearts, a solution containing 0.45 mg/ml of collagenase type II (Worthington, catalog n° 4176) and 1 mg/ml of pancreatin (Sigma, catalog n° P-3292) was used. The supernatants collected during the enzymatic digestion were centrifuged for 10 min at 1000 rpm. The pellet was suspended in isolation medium: DMEM:M199 [4:1] (Thermo Fisher Scientific, catalog n° 41965062 and n° 31150030), 5 % Fetal Bovine Serum (FBS) (Thermo Fisher Scientific, catalog n° A5256701), 10 % Horse serum (HS) (Thermo Fisher Scientific, catalog n° 26050-088), 1 % HEPES (Thermo Fisher Scientific, catalog n° 15630056) and 1 % Penicillin-streptomycin-glutamine (Thermo Fisher Scientific, catalog n° 10378016). Cells were then subjected to three differential platings, of respectively 1 h, 1 h15 and 30 min. All non-adherent cells were removed and resulting rat NVFs attached to the flasks were cultured with fresh isolation medium. After 24 h, the isolation medium was replaced by a fresh maintenance medium (DMEM:M199 [4:1], 5 % of HS and 1 % of Penicillin-streptomycin-glutamine). Under these culture conditions NVFs spontaneously differentiate into neonatal ventricular myofibroblasts (NVMFs) (Fig. S1) [26].

### 2.5. Isolation of cardiac fibroblasts from adult mice

Mouse adult ventricular fibroblasts (AVFs) were extracted from 12 to 14 weeks old C57BL/6J mice using solutions and enzymatic mix from the Pierce Primary Cardiomyocyte Isolation Kit (catalog n° 88281, Thermo Fisher Scientific). Mice were sacrificed by pentobarbital overdose and the heart was removed and washed twice with ice cold Hanks' Balanced Salt Solution (HBSS) without Ca<sup>2+</sup> and Mg<sup>2+</sup>. Ex-vivo heart perfusions were performed by connecting the aorta to a cannula mounted on a syringe filled with HBSS, using a surgical thread. After two initial washes with 1 ml of HBSS, hearts were perfused with 200–300 µl of an enzymatic mix (catalog n° 88281, Thermo Fisher Scientific) and placed in an incubator at 37 °C, 5 % CO<sub>2</sub> for 30 min. Hearts were then incubated with 5 ml of complete culture medium (DMEM supplemented with 10 % of FBS and 1 % of Penicillin-streptomycin-glutamine), cut in small pieces and passed through a 300-µm cell strainer prior being centrifuged at 200 rpm for 3 min. Supernatants were passed through a 40-µm cell strainer and centrifuged at 1000 rpm for 3 min. Pellets were resuspended in complete culture medium and cultured in T-75 flasks coated with 0.2 % gelatin. After 48 h, cells were washed with PBS and fresh culture medium was added. Under

these culture conditions AVFs spontaneously differentiate into adult ventricular myofibroblasts (AVMFs) (Fig. S1) [26].

## 2.6. Immunocytochemistry

Rat NVMFs and mouse AVMFs were seeded in 6 well plates on glass coverslips at  $2 \times 10^5$  cells per well. Cells were fixed with 4 % paraformaldehyde (pre-warmed at 37 °C) for 20 min in a humidified chamber at 37 °C. Cells were then washed with PBS and permeabilized with 0.1 % Triton (Roth, catalog n° 3051.2) for a maximum of 2 min. After three additional washes with PBS, cells were blocked for 1 h in 1 % bovine serum albumin (BSA) (Roth, catalog n° 8076.1). The incubation with primary antibodies was realized in 0.1 % BSA, overnight and at 4 °C. The next day, cells were washed three times in PBS and incubated with secondary antibodies in 0.1 % BSA for 2 h at room temperature. After three final washes with PBS, cells were incubated 30 min with ActinRed™ 555 ReadyProbes™ (Thermo fisher Scientific, catalog n° R37112) prior being mounted on microscopy slides using a mounting medium containing DAPI (Roth, catalog n° HP20.1). Images were acquired using a Zeiss LSM 900 confocal microscope with a Plan-Apochromat 40×/1.30 NA oil immersion objective. The following primaries antibodies were used: mouse monoclonal anti-AKAP2 (custom made, Absolute Antibody, United Kingdom), anti-alpha-smooth muscle actin ( $\alpha$ -SMA) (Sigma, mouse, ref. n° 5228), anti-Arp2 (Abcam, mouse, ref. n° ab49674), anti-ERK1 (Santa Cruz, rabbit, G-8), anti-phospho-ERK (Cell signaling, #4370).

## 2.7. Proximity ligation assays

Rat NVMFs seeded on glass coverslips were fixed using 4 % paraformaldehyde for 20 min in a humidified chamber at 37 °C. Cells were then permeabilized 10 min with 0.1 % Triton-X-100 (Roth, catalog n° 3051.2) at 4 °C and coverslips blocked for 1 in PBS supplemented with 1 % bovine serum albumin (Roth, catalog n° 8076.1). Proximity ligation was performed using the Duolink® Proximity Ligation Assay kit (Merck, DUO92008) according to manufacturer's protocol. F-actin was stained with the Actin Green 488 Ready probe (Invitrogen, catalog n° R37110). Coverslips were mounted on microscope slides using DAPI-containing mounting medium. The following antibodies were used: anti-AKAP2 (custom made, Absolute Antibody, United Kingdom), anti- $\beta$ -actin (Sigma Aldrich, A3853).

## 2.8. Cell culture

Human Embryonic Kidney (HEK) 293 and HEK 293-LTV cells (Cell-Biolabs) were maintained in Dulbecco's Modified Eagle Medium (DMEM) (Thermo Fisher Scientific, catalog n° 41965062) containing 5 % FBS and 100  $\mu$ g/ml of gentamicin (Thermo Fisher Scientific, catalog n° 15750037) in 5 % CO<sub>2</sub> humidified atmosphere at 37 °C.

## 2.9. Lentiviruses production

VSV-G pseudo typed lentiviruses were produced by cotransfecting HEK 293-LTV with 25  $\mu$ g of pSD28-GFP vector containing the cDNAs encoding rat AKAP2 shRNAs or scrambled shRNAs, 16.5  $\mu$ g of pCMVdr8.91 and 7  $\mu$ g of pMD2.VSVG by using the calcium phosphate method. Cell culture medium (DMEM containing 5 % of FBS and 100  $\mu$ g/ml of gentamicin) was replaced 14 h–16 h after transfection with fresh medium. Cell supernatants were collected 36 h to 42 h later, centrifuged at 800 rpm for 10 min and filtered through a 0.22  $\mu$ m filter unit. Lentiviruses were concentrated by ultracentrifugation at 22'000 rpm for 2 h at 4 °C. The resulting pellet was suspended in 200  $\mu$ l of Phosphate-Buffered Saline (PBS). Virus titers were determined by infecting HEK-293 using serial dilution of the viral stock and by scoring the number of GFP-positive colonies, 72 h after infection. Viral titers determined using this method were approximately  $2 \times 10^8$  plaque forming unit

(PFU)/ml.

## 2.10. Lentiviral infection

Rat NVMFs were infected at 50 % confluence using pSD28-based lentiviruses at a multiplicity of infection (MOI) of 15 in maintenance medium supplemented with 8  $\mu$ g/ml of polybrene (Sigma, catalog n° 107689-10G). 72 h after infection, cells were used for experiments.

## 2.11. Wound healing assay

Rat NVMFs seeded at  $5 \times 10^5$  cells per 30 mm dishes were infected with control lentiviruses, or lentiviruses encoding AKAP2 shRNAs or scrambled shRNAs. All lentiviruses also express GFP. 72 h after infection, cells were trypsinized and seeded at  $1.5 \times 10^3$  cells per well in an Incucyte® Imagemock 96-well Plate (Sartorius, ref. n° BA-04856). The remaining cells were kept and used to determine AKAP2 silencing by Western blot. 24 h later, confluent monolayers were wounded using the Incucyte® Wound Maker 96-Tool (Sartorius, ref. n° 4563) and placed in the Incucyte® S3 live cell analysis instrument (Sartorius) for 72 h. The images were acquired every 6 h for a total of 3 days with a 10× objective. The results were analyzed using the Incucyte® Scratch Wound Analysis Software Module (Sartorius, ref. n° 9600-0012).

## 2.12. Proliferation

$5 \times 10^5$  rat NVMFs were seeded in 15 mm dishes and infected with control lentiviruses, or lentiviruses encoding AKAP2 shRNAs or scrambled shRNAs. All lentiviruses also express GFP. 72 h after infection, plates were placed in an Incucyte S3 instrument (Sartorius) and the images were acquired after 24 h with a 10× objective. The number of GFP positive cardiac myofibroblasts was analyzed with the Incucyte® Base Software Module (Sartorius).

## 2.13. SDS-PAGE and Western blotting

Rat NVFs were lysed in radio-immunoprecipitation assay buffer (RIPA) (Merk, catalog n° R0278) or in buffer A (20 mM Tris pH 7.4, 150 mM NaCl, 1 % Triton-X-100, supplemented with protease and phosphatase inhibitors (Thermo Fisher Scientific, catalog n° 78447)). Samples were denatured in SDS-PAGE buffer (65 mM Tris-HCl pH 6.8, 2 % SDS, 5 % glycerol, 5 % 2-mercaptoethanol) at 95 °C for 5 min and separated on acrylamide gels prior being electro-blotted onto nitrocellulose membranes. Membranes were blocked for 1 h in 5 % of non-fat milk (or in Horse serum for the actin overlay) and subsequently incubated with primary antibodies overnight at 4 °C and horseradish peroxidase (HRP)-conjugated secondary antibodies for 1 h30 at room temperature. The following primary antibodies were used for immunoblotting: mouse monoclonal anti-AKAP2 (custom made, Absolute Antibody, United Kingdom), anti-GAPDH (Abcam, rabbit, ref. n° ab181602), anti-ERK1 (Santa Cruz, rabbit, G-8), anti-phospho-ERK (Cell signaling, #4370), anti-Grb2 (Abcam, rabbit, ref. n° ab32111), anti-WAVE 2 (Cell signaling, #3659), anti-phospho-WAVE2 (Sigma, ref. n° 07-1512), anti-Filamin A (Cell signaling, #4762), anti-phospho-Filamin A (Cell signaling, #4761), anti-SAPK/JNK (Cell signaling, #9252), anti-phospho-SAPK/JNK (Cell signaling, #4668), anti-phospho-p38 (Cell signaling, #9211), anti-p38 (Cell signaling, #9212). Protein expression was quantified by densitometry using ImageJ software.

## 2.14. AKAP2 immunoprecipitation

Endogenous AKAP2 was immunoprecipitated from rat NVFs. Cells were grown in 100 mm dishes and lysed in buffer D (50 mM Tris-HCl pH 7.5, 1 % Triton-100×, 1 mM DTT) and proteases inhibitors (Thermo Fisher Scientific, catalog n. A32963). Cell lysates were incubated 2 h at 4 °C on a rotating wheel and then centrifuged at 14'000 rpm

for 20 min at 4 °C. Protein content of cell lysates was quantified using the DC Protein assay (BioRad, catalog n° 500–0111). 1.5 mg/ml of lysate proteins were incubated overnight at 4 °C on a wheel with 2 µg of mouse anti-AKAP2 antibodies (Custom made, Absolute Antibody Ltd) or with 2 µg of rabbit anti-AKAP2 antibodies (custom made, Covance, San Diego, CA, USA). Lysates were incubated with protein-G Sepharose beads (Thermo Fisher Scientific, catalog n° 10-1242) for 4 h at 4 °C on a rotating wheel. Following a brief benchtop centrifugation, beads were washed twice with a lysis buffer E (20 mM Tris pH 7.4, 250 mM NaCl, 1 % Triton-100×, and proteases inhibitors) and then twice with a lysis buffer F (20 mM Tris pH 7.4, 150 mM NaCl, 1 % Triton-100× and proteases inhibitors). Proteins were eluted in SDS-PAGE loading buffer (50 mM Tris pH 6.8, 2 % SDS, 5 % 2-mercaptoethanol, 10 % glycerol, 0,1 % bromophenol blue) by boiling samples for 5 min at 95 °C. Proteins eluted from the beads were analyzed by SDS-PAGE and Western blotting.

### 2.15. Mass spectrometry analysis and protein identification

Mass spectrometry was performed by the Protein Analysis Facility of the University of Lausanne. All immunoprecipitated proteins were extracted from beads by boiling in 50 µl of SDS-PAGE loading buffer. Proteins were separated by 1D mini-PAGE over 2.0 cm and stained with Coomassie blue. Entire gel lanes were excised into 5 equal regions from top to bottom and digested with trypsin (Promega #V5073) as described [27]. Data-dependent LC-MS/MS analysis of extracted peptide mixtures after digestion was carried out on a TIMS-TOF Pro (Bruker, Bremen, Germany) mass spectrometer interfaced through a nanospray ion source to an Ultimate 3000 RSLCnano HPLC system (Dionex). Peptides were separated on a reversed-phase custom packed 45 cm C18 column (75 µm ID, 100 Å, Reprosil Pur 1.9 µm particles, Dr. Maisch, Germany) at a flow rate of 0.250 µl/min with a 6–27 % acetonitrile gradient in 92 min followed by a ramp to 45 % in 15 min and to 95 % in 5 min (all solvents contained 0.1 % formic acid). Data-dependent acquisition of peptide tandem mass spectra was carried out using the standard PASEF method [28].

Data files were analyzed with MaxQuant 1.6.14.0 [29] incorporating the Andromeda search engine [30]. Cysteine carbamidomethylation was selected as fixed modification while methionine oxidation and protein N-terminal acetylation were specified as variable modifications. The sequence databases used for searching were the rat (*Rattus norvegicus*) reference proteome based on the UniProt database ([www.uniprot.org](http://www.uniprot.org), version of May 30th, 2021, containing 29'935 sequences), and a “contaminant” database containing the most usual environmental contaminants and enzymes used for digestion (keratins, trypsin, etc.). Mass tolerance was 4.5 ppm on precursors (after recalibration) and 20 ppm on HCD fragments. Both peptide and protein identifications were filtered at 1 % FDR relative to hits against a decoy database built by reversing protein sequences. Data from all gel bands for each sample were merged to yield the quantitative values. Quantitative protein analysis was based on iBAQ values [31]. Data filtering, analysis and annotation were done with the Perseus package [32,33]. The mass spectrometry proteomics data have been deposited to the ProteomeXchange Consortium via the PRIDE [34] partner repository with the dataset identifier PXD040656.

### 2.16. Bioinformatic analysis of AKAP2 interactome

Proteins detected by mass spectrometry were filtered to consider only specific proteins, significantly enriched in AKAP2 immunoprecipitations over control immunoprecipitations. Enrichment of the proteins was analyzed using Welch's *t*-test difference values. To identify the functional properties of AKAP2-interacting proteins DAVID software was used [35]. Proteins were further grouped in 8 different functional clusters. To find all proteins involved in the regulation of actin cytoskeleton, GOBP, GOMF and KEGG databases were used in addition to manual literature search. The protein interaction map was generated

using Cytoscape version 3.9.1. Existing protein-protein interaction data was used to enrich interaction network of AKAP2. StringApp in Cytoscape was used to merge the experimental data with the STRING database to show interactions also between AKAP2 associated proteins.

### 2.17. Constitutively active ERK1 rescue experiments

Rat NVMFs seeded in 30 mm dishes were infected at 50 % confluence using pSD28-based lentiviruses encoding rat AKAP2 shRNA-1 or scrambled rat AKAP2 shRNA at a MOI of 15 in maintenance medium supplemented with 8 µg/ml of polybrene (Sigma, catalog n° 107689-10G). 24 h after infection, cells were transfected with 4 µg of the pFlag-ERK1 R84S construct using Lipofectamine 2000 according to the manufacturer's protocol (ThermoFisher, 11668027). 48 h after transfection cells were used for experiments.

### 2.18. Expression and purification of glutathione-S-transferase (GST) fusion proteins

GST-tagged fusion proteins of the AKAP2 fragment encompassing residues 331 to 491 and of the Rho binding domain (RBD) of Rhotekin were expressed using the bacterial expression vector pGEX4T1 in the BL21DE3 strain of *Escherichia coli* and purified. To induce the expression of fusion proteins, exponentially growing bacterial cultures were incubated 16 h at 16 °C with 1 mM isopropyl 1-thio-β-D-galactopyranoside (IPTG), and subsequently subjected to centrifugation at 4'000 ×g at 4 °C. Pelleted bacteria were lysed in buffer B (20 mM Tris pH 7.4, 150 mM NaCl, 5 mM MgCl<sub>2</sub>, 1 % Triton 100×), and protease inhibitors (Thermo Fisher Scientific, catalog n. A32963), sonicated, and centrifuged at 10,000 ×g for 30 min at 4 °C. After incubating the supernatants with glutathione Sepharose beads (Cytiva, catalog n° 17075601) for 2 h at 4 °C, the resin was washed three times with 10 volumes of buffer C (20 mM Tris pH 7.4, 300 mM NaCl, 1 % Triton 100×, and protease inhibitors). The protein content of the beads was assessed by Coomassie Blue staining of SDS-polyacrylamide gels. Beads were finally stored at –20 °C.

### 2.19. Cell permeant competitor peptides

Competitor peptides disrupting the interaction between AKAP2 and F-actin (R<sub>11</sub>-EQIDFSAARKQFQQMENSQRQT) and scrambled competitor peptides (R<sub>11</sub>-MFSRSQNFQIREAADQKQETQ) were synthesized by Bachem (Dübendorf, Switzerland). Peptides were rendered cell permeant by the addition of N-terminal tails of 11 arginines. Lyophilized peptides were dissolved in water and stored at –80 °C.

### 2.20. Solid phase F-actin overlay assay

Filamentous Actin (F-actin) was produced as it follows: non-muscle actin (Cytoskeleton Inc., catalog n° APHL99) was resuspended in 250 µl of general actin buffer (Cytoskeleton Inc., catalog n° BSA01-001) supplemented with 0,2 mM ATP (Cytoskeleton Inc., catalog n° BSA04-001) for 1 h on ice. 25 µl of actin polymerization buffer (Cytoskeleton Inc., catalog n° BSA02-001) were added to the depolymerized actin protein prepared as indicated above and incubated for 1 h at 24 °C. This represents the F-Actin stock at 21 µM to be used for F-actin overlay assays. GST-AKAP2 331-491 fragments containing the actin binding site were electro-blotted onto nitrocellulose membranes. Membranes were blocked for 1 h at room temperature with Horse Serum (Thermo Fisher Scientific, catalog n° 26050-088) and subsequently incubated with or without F-Actin at 1 µM, in the absence or presence of 10 µM, 20 µM or 50 µM of competitor or scrambled competitor peptides overnight at room temperature. After three washes in TBS-Tween, the blots were incubated for 2 h with HRP-conjugated anti-actin antibodies (Cell Signaling, #12620, dilution 1:5000) in TBS-Tween. Membranes were then washed three times in TBS-Tween and subjected to

autoradiography.

### 2.21. Time-lapse microscopy and cell tracking

Rat neonatal cardiac myofibroblasts seeded at  $5 \times 10^5$  cells per 30 mm dish were infected with the appropriate lentiviruses. 72 h after infection, cells were trypsinized and seeded at  $1 \times 10^5$  cells per  $\mu$ -Slide I (Ibidi, catalog n° 80106). The remaining cells were kept and used to determine AKAP2 silencing by Western blot. 4 h after seeding, cells were placed on a Spinning Disk microscope (Nikon Ti2, Yokogawa CSU-W1) in a live cell imaging culture chamber at 5 % CO<sub>2</sub> and 37 °C. Images were acquired every 10 min for 24 h with a CFI Plan Apochromat Lambda 40XC objective (N.A. 0.95, W.D. 0.21 mm, Spring-loaded, Cover glass correction: 0.11–0.23 mm). Data were analyzed and plotted with the Tracking Tool Pro v2.1 from Gradientech.

### 2.22. Analysis of phospho-ERK and ARP2 subcellular distribution in cardiac myofibroblasts

For the analysis of phospho-ERK subcellular distribution, rat NVMFs seeded in 30 mm dishes were infected at 50 % confluence using pSD28-based lentiviruses encoding rat AKAP2 shRNA-1 or scrambled rat AKAP2 shRNA at a MOI of 15 in maintenance medium supplemented with 8  $\mu$ g/ml of polybrene (Sigma, catalog n° 107689-10G). 72 h after infection, cells were stained for phospho-ERK and  $\alpha$ -SMA as indicated in the protocol for immunocytochemistry described above. The phospho-ERK fluorescence intensity was averaged from 60  $\mu$ m wide bands perpendicular to the cell edge and towards the nucleus by using the ImageJ software. Images were obtained from 3 independent experiments with  $n = 5$  cells analyzed per condition. For the analysis of ARP2 subcellular distribution,  $6 \times 10^4$  rat NVMFs seeded in 15 mm wells were incubated with 20  $\mu$ M of R<sub>11</sub>-AKAP2 319-342 or scrambled R<sub>11</sub>-AKAP2 319-342 peptides for 1 h. Cells were stained for Arp2 and actin as indicated in the protocol for immunocytochemistry described above. The Arp2 fluorescence intensity was averaged from 3  $\mu$ m wide bands perpendicular to the cell edge and towards the cell center by using the ImageJ software. Images were obtained from 3 independent experiments with  $n = 10$  cells analyzed per condition.

### 2.23. RBD and Cdc42/Rac1-binding motif (CRIB) pull-down assays

Rat NVMFs grown in 100 mm dishes were lysed in RBD lysis buffer (20 mM Tris pH 7.4, 150 mM NaCl, 1 % (w/v), Triton-X-100, 0.1 % sodium deoxycholate, 30 mM MgCl<sub>2</sub>, 1 mM DTT, 10 % glycerol, 1 mM benzamidine, 10  $\mu$ g/ml leupeptin, 10  $\mu$ g/ml aprotinin, 1 mM PMSF). Lysates were subjected to centrifugation at 38,000  $\times$ g for 10 min at 4 °C and incubated with 40  $\mu$ g of RBD or CRIB beads (Cytoskeleton, catalog n° PAK01-A) for 1 h at 4 °C. Beads were then washed three times with RBD buffer without sodium deoxycholate, resuspended in SDS-sample buffer, separated on acrylamide gels and electroblotted onto nitrocellulose membranes. The blots were incubated with anti-RhoA (Santa Cruz, catalog n° sc-418, 200  $\mu$ g/ml, 1:500 dilution), anti-Rac1 (BD Biosciences, catalog n° 610651, 1:1000 dilution), or anti-Cdc42 antibodies (Santa Cruz, catalog n° sc-8401, 200  $\mu$ g/ml, 1:250 dilution) and subsequently with horseradish-conjugated secondary antibodies.

### 2.24. Statistical analysis

All values presented in the figures are mean  $\pm$  standard error of the mean (SEM). Differences among multiple groups were analyzed with 1 or 2-way Brown-Forsythe Anova test followed by Dunnett's T3 multiple comparison test, with individual variance computed for each comparison. Difference in means between two groups were analyzed by unpaired *t*-test with Welch's correction. All statistics were performed with the GraphPad Prism Software 9.5.1 version. Values of  $p < 0.05$  and below were considered statistically significant.

## 3. Results

### 3.1. AKAP2 is expressed in cardiac myofibroblasts

While recent evidence indicates that AKAP2 activates cardioprotective pathways in cardiomyocytes that attenuate myocardial damage and remodeling in response to cardiac stress [25], it is currently unknown whether this anchoring protein can exert specific functions in cardiac cells other than cardiomyocytes.

To address this question, we characterized AKAP2 distribution in cardiac cells of healthy and stressed hearts. AKAP2 expression and localization was initially examined in the heart of mice subjected to sham surgery or permanent occlusion of the left anterior descending coronary artery (LAD), which causes infarction of the anterior wall of the left ventricle. Immunostaining of transversal heart sections revealed an increased expression of AKAP2 in the infarcted area (Fig. 1A, lower panels), which is mainly composed of collagen fibers and non-myocyte cells. Basal AKAP2 expression was also detected in the healthy myocardium (Fig. 1A). To identify the non-myocyte cell population expressing AKAP2, heart sections were co-stained using different cell-specific markers including  $\alpha$ -SMA, which labels cardiac myofibroblasts and smooth muscle cell in the tunica media of blood vessels; vimentin, which is enriched in cardiac fibroblasts; and laminin, which stains basement membranes of all cardiac cells. In sham-operated animals, AKAP2 expression was detected in interstitial cells of the myocardium and in endothelial cells in the inner layer of blood vessels (Fig. 1B and C). In mice subjected to MI, we detected increased AKAP2 expression in cardiomyocytes located in the area surrounding the infarcted zone, confirming previous findings [25], but also in  $\alpha$ -SMA- and vimentin-positive fibroblasts (Fig. 1D and E). Quantitation of AKAP2 stainings revealed that 55 % of the  $\alpha$ -SMA-positive fibroblasts and 75 % of the vimentin-positive fibroblasts express AKAP2. These findings indicate that AKAP2 is expressed in multiple cardiac cell types, including myofibroblasts that are induced in response to cardiac stress.

### 3.2. AKAP2 interacts with actin and mediates cardiac myofibroblast migration

Given the crucial role of cardiac myofibroblasts in the process of cardiac remodeling, we sought to gain more insights into the function of AKAP2 in these cardiac cells. To address this aspect, we first assessed the subcellular localization of AKAP2 in primary cultures of cardiac myofibroblasts from neonatal rats or adult mice. Both primary cultures were shown to express vimentin and  $\alpha$ -SMA suggesting that fibroblasts underwent differentiation to myofibroblasts (Suppl. Fig. 1). As shown in Fig. 2A, immunolabeling experiments revealed an enrichment of AKAP2 at lamellipodia forming at the leading edge of migrating cells [12]. Since lamellipodia are mainly constituted by branched actin filaments, we determined whether AKAP2 forms complexes with actin at these subcellular sites using proximity ligation assays (PLA). A polarized subcellular distribution of AKAP2-actin complexes at the leading edge was detected in rat neonatal ventricular myofibroblasts (NVMF) incubated with both AKAP2 and actin antibodies (Fig. 2B, right panel, and Fig. 2C and D). In control experiments (Ctrl), performed by individually incubating cells with AKAP2 antibodies, no signal was detected (Fig. 2B, left panel, and Fig. 2D).

Lamellipodia extension through local rearrangements of the actin cytoskeleton provides the driving force for migration [13]. Based on this evidence, we raised the possibility that AKAP2 interaction with actin might regulate the migratory capacity of cardiac myofibroblasts. To address this hypothesis, we investigated the impact of AKAP2 knockdown on myofibroblast migration using a wound healing assay. Rat NVMFs were infected with lentiviruses encoding AKAP2-specific shRNAs (shRNA1 and 2), a scrambled AKAP2 shRNA (sc shRNA) or a control lentivirus expressing no shRNA. Our results indicate that knockdown of AKAP2 expression using two independent shRNAs

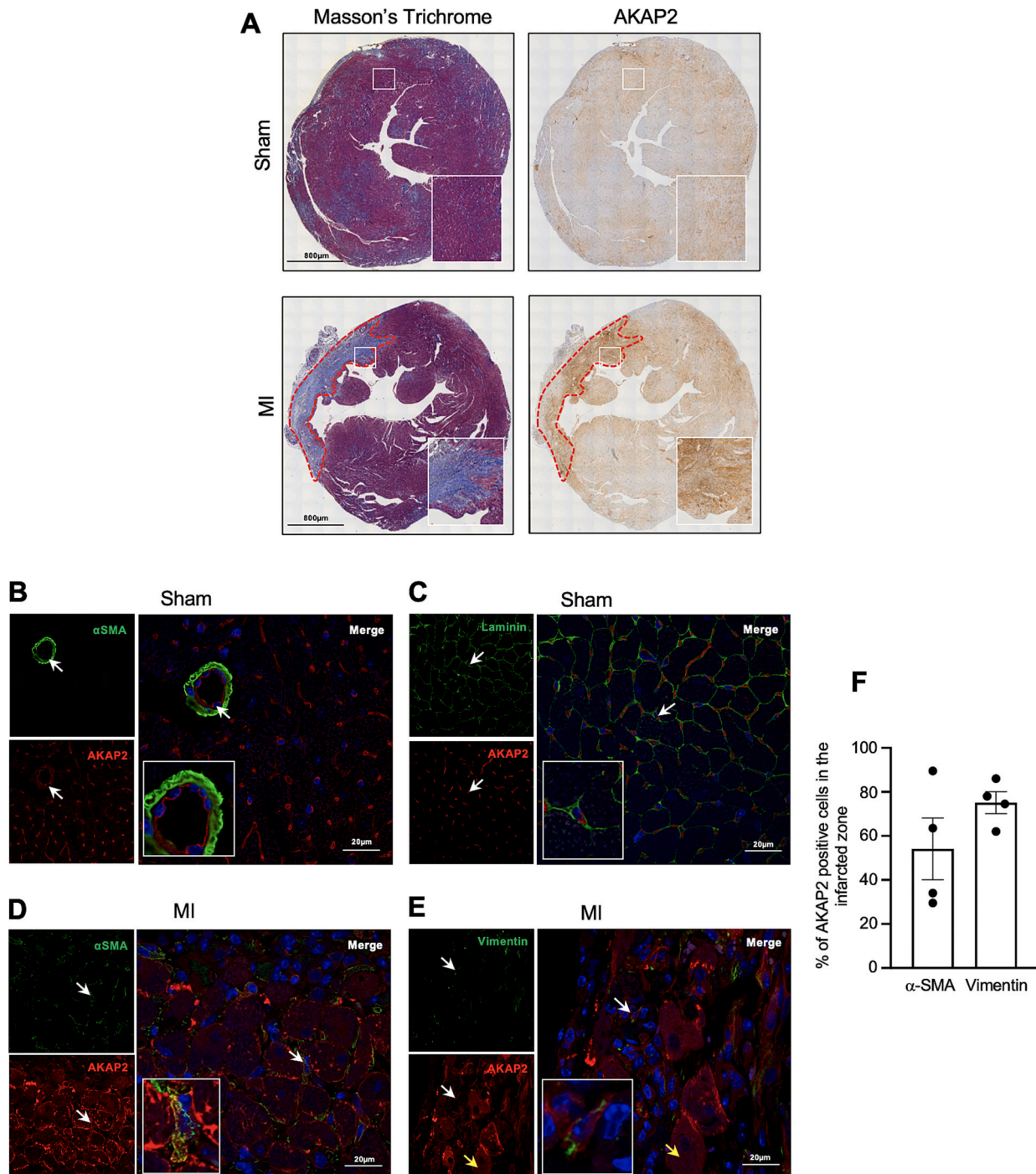
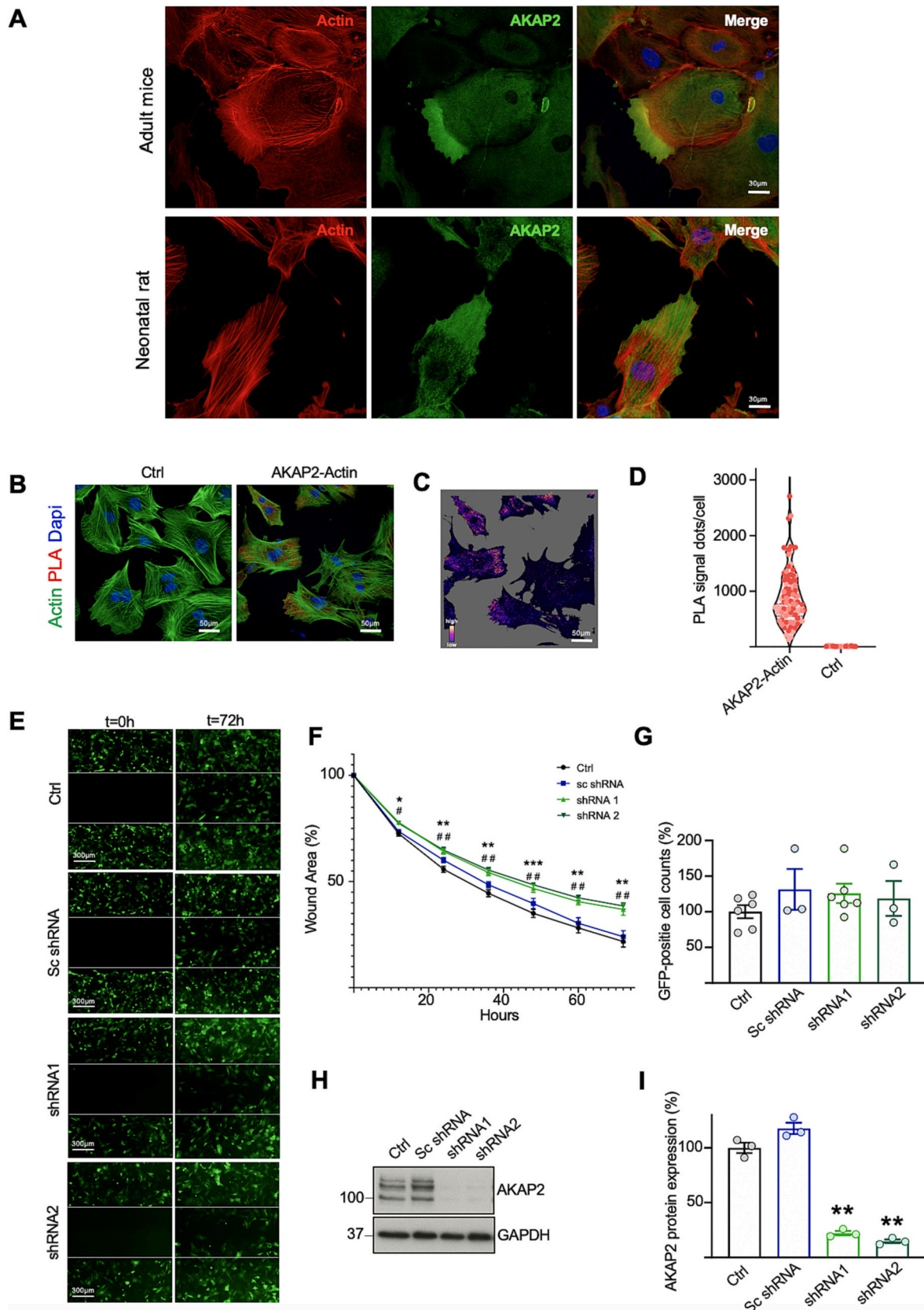


**Fig. 1.** AKAP2 expression is increased in cardiac myofibroblasts after myocardial infarction. **A**) Masson's Trichrome (left panel) and AKAP2 (right panel) staining of transversal ventricular sections from mice subjected to sham operation or LAD ligation (MI) for 2 weeks. The boundary between infarcted (IZ) and border zone (BZ) is indicated by a red dotted line. Magnifications of myocardial regions in dashed squares are shown in the lower right corner. **B–E**) Immunohistochemical analysis of AKAP2 expressing cells in myocardial tissues from mice subjected to sham operation or LAD ligation (MI) for 2 weeks. Transversal ventricular sections were co-stained with anti-AKAP2 (red) and anti- $\alpha$ SMA (green) (**B**, **D**), anti-laminin (**C**) or anti-vimentin antibodies (**E**). Nuclei were visualized with DAPI. White arrows indicate co-staining in non-myocyte cells. The yellow arrow highlights AKAP2 expression in cardiomyocytes. **F**) Percentage of  $\alpha$ -SMA-positive and vimentin-positive fibroblasts expressing AKAP2 within the infarcted zone. Results are presented as mean  $\pm$  S.E. ( $n = 4$ ).

(**Fig. 2H** and **I**) significantly impairs wound healing (**Fig. 2E** and **F**). Since, AKAP2 silencing does not impact rat NVMF proliferation (**Fig. 2G**), the reduction of the ability of rat NVMF to close the wound can be attributed to an inhibition of migration. Taken together, these findings suggest that AKAP2 colocalizes with the actin cytoskeleton at the lamellipodia of migrating myofibroblasts and that the absence of AKAP2 reduces the ability of these cardiac cells to migrate.

### 3.3. AKAP2 assembles an ERK1-based signaling complex

To gain insight into the molecular mechanism whereby AKAP2 affects cell migration, we performed a proteomic analysis of AKAP2-interacting proteins in cardiac myofibroblasts. To this end, AKAP2 was immunoprecipitated from rat NVMFs lysates and AKAP2 immunoprecipitates were analyzed by shotgun mass spectrometry (**Fig. 3A** and **B**).



(caption on next page)

**Fig. 2.** AKAP2 interacts with actin and promotes myfibroblasts migration. A) Primary cultures of mouse AVMFs (upper panels) and rat NVMFs (lower panels) were fixed, permeabilized and incubated with LifeAct to visualize F-actin (red) and anti-AKAP2 antibodies as well as AlexaFluor488-conjugated anti-mouse secondary antibodies to detect the expression of AKAP2. B) Proximity ligation assay for rat NVMFs incubated with anti-AKAP2 and anti-actin antibodies alone or in combination. Nuclei were stained with DAPI and shown in blue whereas F-actin was stained with the Actin Green Ready probe. PLA signals representing positive AKAP2/actin interactions are shown in red. C) Signal intensity projection of PLA dots detected in rat NVMFs incubated with both anti-AKAP2 and anti-actin antibodies. D) Quantification of the PLA fluorescent signal per cell using ImageJ. Results are expressed as mean  $\pm$  S.E. of 3 independent experiments. Approximately 25 cells were analyzed per experiment. E) Wounded monolayers of rat NVMFs were infected with lentiviruses encoding shRNAs against AKAP2 (shRNA1 and shRNA2) or control lentiviruses (Ctrl and sc shRNA). All lentiviruses also encode GFP to allow visualization of infected cells. Recolonization of the wounded area was imaged every 2 h for a total of 72 h. Scale bar, 300  $\mu$ m. F) Quantitation of the wound-healing process. Wound closure is expressed as percentage of the wound surface at 0 h. Results are presented as mean  $\pm$  S.E. of 6 independent experiments. \* and # $p$  < 0.05, \*\* and ## $p$  < 0.005, \*\*\* and ### $p$  < 0.0005 compared with the wounded area measured in monolayers transfected with control shRNAs. G)  $2 \times 10^4$  rat NVMFs infected as indicated in E) were seeded on 15 mm wells. 72 h after infection GFP positive cells were analyzed using the Incucyte® Base Software Module. Results are presented as mean  $\pm$  S.E. of 3 to 6 independent experiments. H) Western blot analysis of AKAP2 expression in rat NVFs infected with control (Ctrl) shRNA, shRNA1 or shRNA2. I) Quantitative analysis of AKAP2 expression in rat NVMFs cell lysates was obtained by densitometry. The amount of AKAP2 was normalized to GAPDH. Results are expressed as mean  $\pm$  S.E. of 3 independent experiments: \*\* $p$  < 0.005.

The most represented binding partners identified using this approach were regulators of the actin cytoskeleton (26 % of the interactors) and proteins regulating intracellular membrane trafficking or vesicle-mediated trafficking (22 % of the interactors) (Fig. 3C and D).

Pathway analysis of the AKAP2 interactors known to modulate the actin cytoskeleton identified two components of extracellular signal-regulated kinase 1 (ERK1) signaling cascade including the adaptor protein growth factor receptor-bound protein 2 (Grb2) and ERK1 (also known as mitogen activated protein kinase 3 (MAPK3)) (Fig. 3D and E). Importantly the ERK signaling pathway has been shown to regulate cell motility independently of its function in regulating gene expression [36]. In particular, ERK 1/2 enhances the function of various regulators of actin remodeling and migration at the cell the leading edge including the WAVE2-Arp2/3 transduction pathway, which promotes branched actin polymerization [17] and the ribosomal S6 kinase (RSK)-filamin A signaling axis, which favors cell motility by inhibiting focal adhesion assembly [37] (Fig. 3E).

To confirm the binding between AKAP2, Grb2 and ERK1 in cardiac myofibroblasts, lysates from rat NVMFs were subjected to immunoprecipitation using antibodies against AKAP2 or control mouse IgGs. Western blot analysis of the coimmunoprecipitated proteins revealed the presence of Grb2 and ERK1, suggesting that these two components of the ERK pathway form a complex with endogenous AKAP2 in cardiac myofibroblasts (Fig. 3F). Immunolabeling experiments revealed colocalization of AKAP2 and ERK1 at the leading edge of migrating cells, as well as in intracellular regions (Fig. 3G). Collectively, these findings raise the hypothesis that AKAP2-ERK1 signaling complexes might regulate pro-migratory pathways at the leading edge of cardiac myofibroblasts.

### 3.4. AKAP2 promotes phosphorylation of ERK1 and WAVE2 in cardiac myofibroblasts

By locally recruiting signaling enzymes and regulators, anchoring proteins facilitate efficient activation of transduction pathways [19]. In this context, our findings that AKAP2 recruits key molecules of the ERK cascade suggest that this anchoring protein might contribute to the activation of ERK and its downstream effectors in cardiac myofibroblasts. To investigate this aspect, we first determined whether AKAP2 knockdown in rat NVMFs could affect the activation of ERK1/2 and its downstream effectors, WAVE2 and filamin A, involved in actin remodeling.

Rat NVMFs were infected with lentiviruses encoding AKAP2-specific shRNAs, scrambled shRNAs or control lentiviruses (Ctrl). Activation of ERK1/2, WAVE2 and the RSK-filamin A signaling axis was assessed by Western blot using antibodies recognizing phosphothreonine 202 and phosphotyrosine 204 of ERK, phosphoserine 343 of WAVE2 and phosphoserine 2152 of filamin A, respectively (Fig. 4). Our results indicate that AKAP2 silencing reduces by 50 to 60 % the phosphorylation of ERK1/2 (Fig. 4A and B) and WAVE2 (Fig. 4A and C), without affecting filamin A phosphorylation (Fig. 4A and D). This suggests that, in cardiac

myofibroblasts, AKAP2 mediates the activation of ERK1/2 and its downstream effector WAVE2 but is not directly involved in the ERK-mediated regulation of filamin A.

To further investigate AKAP2-mediated ERK1 phosphorylation in cardiac myofibroblasts, we immunostained rat NVMFs expressing wild type or scrambled AKAP2 shRNAs using anti-phospho-ERK antibodies. We could observe a 44,5 % reduction of the phospho-ERK levels in a cellular area that extends from the leading edge to the nucleus (Fig. 4E and F). These findings suggest that AKAP2 regulates ERK1 phosphorylation in different cellular compartments and are consistent with our results indicating that AKAP2 and ERK1 colocalize both at the leading edge and in intracellular regions (Fig. 3G).

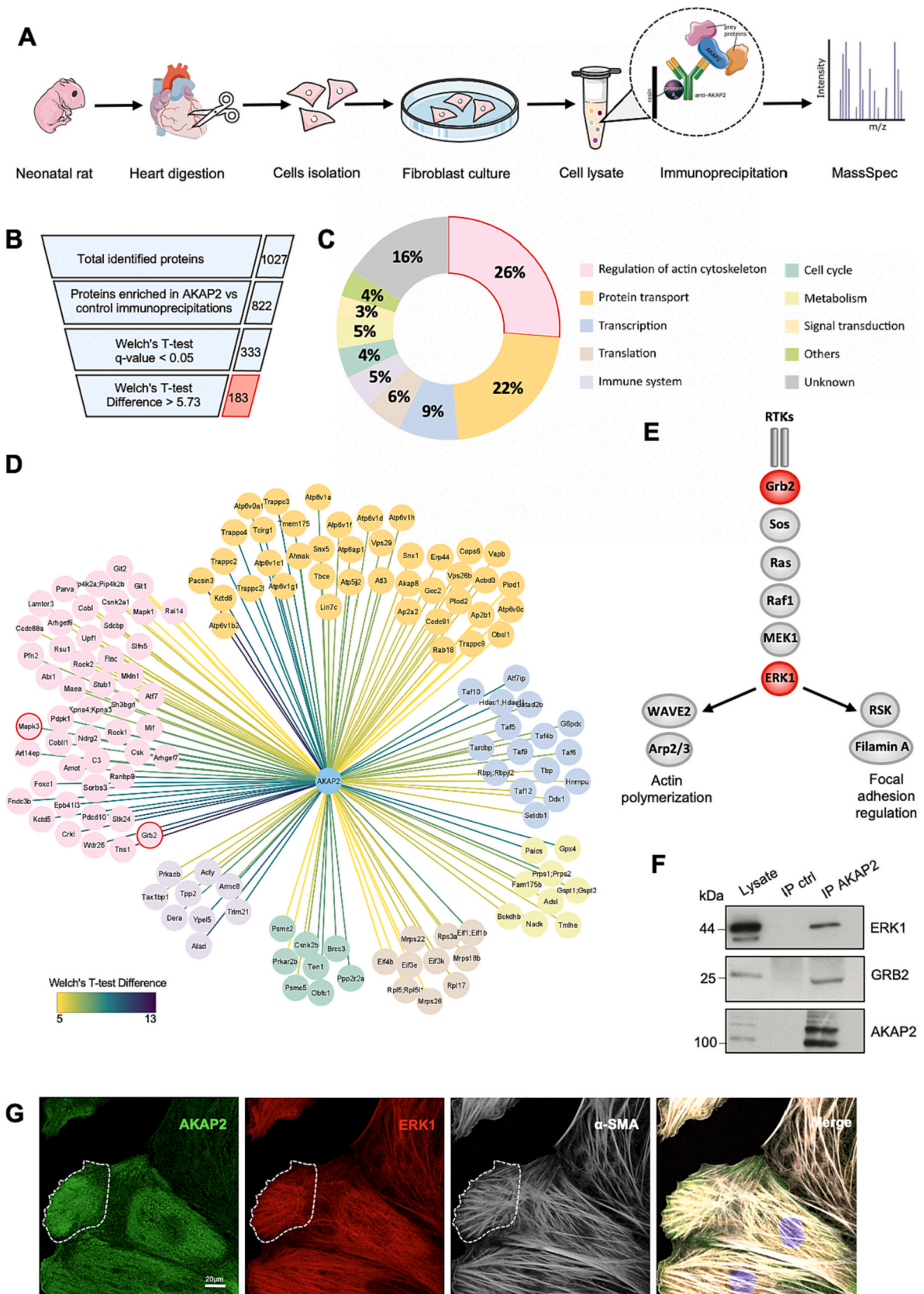
Finally, we could provide evidence that ERK1 regulates WAVE2 phosphorylation downstream of AKAP2, as shown by the fact that expression of a Flag-tagged constitutive active mutant of ERK1 (Flag-ERK1 R84S) in AKAP2 silenced rat NVMFs restores WAVE2 phosphorylation on serine 343 (Fig. 4G and H).

### 3.5. Generation of a competitor peptide disrupting the AKAP2/F-actin interaction

We recently showed that AKAP2 interacts with F-actin through a binding site located between residues 319 and 341 of the anchoring protein [38]. This interaction motif (EQIDFSAARKQFQQMENSQRQT) differs from previously identified actin binding sites since F-actin interaction is mainly mediated by phenylalanine and arginine residues within the motif [38].

To determine whether the F-actin binding domain of AKAP2 functions as a competitive inhibitor of the interaction between the anchoring protein and F-actin, we generated cell-permeant competitor peptides (R<sub>11</sub>-AKAP2 319-342) and control scrambled peptides (R<sub>11</sub>-AKAP2 319-342 scrambled) by fusing a poly-arginine tail to the N-terminus of the peptides. Peptides usually lack cell permeability, which prevents their intracellular delivery. In this context the addition of poly-arginine tails allows peptides to cross the plasma membrane. This strategy has been used previously to successfully to generate cell-penetrant peptides disrupting the interaction between AKAPs and PKA regulatory subunits [39–41].

We subsequently determined the impact of increasing concentrations of R<sub>11</sub>-AKAP2 319-342 peptides (10  $\mu$ M, 20  $\mu$ M, and 50  $\mu$ M) on the ability of purified F-actin to bind a GST fragment of AKAP2 containing the actin binding site immobilized onto a nitrocellulose membrane. F-actin binding to AKAP2 was detected by immunoblot using an HRP-conjugated anti-actin antibody. Our results indicate that F-actin binding was inhibited by approximately 60 % at a concentration of peptide of 10  $\mu$ M and completely abolished at concentrations above 20  $\mu$ M (Fig. 5A, upper panels, and B). In control experiments, the presence of comparable concentrations of scrambled peptides did not affect the interaction between F-actin and the AKAP2 fragment (Fig. 5A upper panels, and B). These results suggest that the R<sub>11</sub>-AKAP2 319-342 peptide competitively inhibits the interaction between AKAP2 and F-actin.



(caption on next page)

**Fig. 3.** Quantitative mass spectrometry identifies AKAP2 interactome. A) Schematic representation of the immunoprecipitation–mass spectrometry approach used to identify the AKAP2 interactome in cardiac myofibroblasts. AKAP2 was immunoprecipitated from primary cultures of rat NVMFs and AKAP2 immunoprecipitates were subsequently analyzed by shotgun LC–MS/MS mass spectrometry to identify AKAP2-interacting proteins. The figure was created using the vector image bank of Servier Medical Art licensed under a Creative Common Attribution 3.0 Generic License. B) Analysis workflow for the filtering of mass spectrometry data. Only proteins significantly enriched in AKAP2 immunoprecipitates over control immunoprecipitations with rabbit IgGs with the cut-off of 5.73 for Welch's *t*-test difference were further analyzed. Filtering resulted in a final dataset of 183 proteins. C) AKAP2 interacting protein distribution by assigned category. Pie chart showing the distribution of a total number of 183 mass spectrometry-identified proteins in AKAP2 immunoprecipitates from rat NVMFs. D) AKAP2 interacting proteins grouped based on their function and presented as a network. The colors of the nodes represent assignment to specific functional group (colored according to the legend). Only chosen groups were presented in the network. Colors of the edges from nodes mark the enrichment (Welch's *t*-test difference) of proteins in AKAP2 vs control immunoprecipitations. E) Schematic representation of the ERK signaling pathway controlling actin cytoskeleton remodeling and cell migration [17,37]. Proteins identified in AKAP2 immunoprecipitates are highlighted in red. F) Rat NVMFs were subjected to immunoprecipitation with non-immune mouse IgG or anti-AKAP2 monoclonal antibodies. Western blot of the immunoprecipitates were revealed with anti-ERK1 (upper panel), anti-Grb2 and anti-AKAP2 antibodies (lower panel). G) Rat NVMFs were fixed, permeabilized and co-stained with anti-AKAP2 (green), anti-ERK1 (red), and anti- $\alpha$ SMA (gray) antibodies. The cell leading edge is highlighted by a dashed white line.

### 3.6. Tethering AKAP2 to F-actin contributes to the activation of the ERK1-WAVE2 pathway in cardiac myofibroblasts

To determine whether the recruitment of the AKAP2/ERK1 complex to the actin cytoskeleton mediates the activation of the ERK-WAVE2 transduction cascade, we assessed the impact of disrupting the AKAP2-F-actin interaction using competitor peptides on the activation of ERK1/2 and WAVE2 in cardiac myofibroblasts (Fig. 6A). Incubation of rat NVMFs with 20  $\mu$ M of R<sub>11</sub>-AKAP2 319-342 for 1 h reduced by 50 % to 60 % the phosphorylation of ERK and WAVE2, whereas scrambled R<sub>11</sub>-AKAP2 319-342 had no impact on ERK1/2 and WAVE2 phosphorylation (Fig. 6B–D). The decrease in ERK phosphorylation induced by the R<sub>11</sub>-AKAP2 319-342 cannot be attributed to a non-specific inhibition of the interaction between AKAP2 and ERK1, since incubation of rat NVMFs with 20  $\mu$ M of the competitor peptide did not alter the capacity of ERK1 to co-immunoprecipitate with AKAP2 (Fig. S2). In line with our findings showing that AKAP2 does not regulate filamin A (Fig. 4), the AKAP2-F-actin competitor did not affect filamin A phosphorylation (Fig. 6B and E).

Several studies have shown that in addition to ERK, other MAPKs including Jun N-terminal kinase (JNK) and p38, can also regulate cell migration [36]. In this context, control experiments revealed that the R<sub>11</sub>-AKAP2 319-342 peptide did not perturb phosphorylation levels of additional MAPKs known to regulate cell migration, including JNK and p38 (Fig. 6B and F and G). Taken together these results indicate that the activation of the ERK-WAVE2 signaling pathway (but not that of the JNK and p38 transduction cascades) is dependent on the direct interaction of AKAP2 with the actin cytoskeleton.

### 3.7. Tethering AKAP2 to F-actin favors ARP2 localization at the cardiac myofibroblast leading edge and cell migration

The Arp2/3 complex is a key regulator of branched F-actin nucleation at the leading edge [42]. Its activity is enhanced by direct interaction with nucleation-promoting factors (NPFs) such as WAVE2 [15]. Previous findings have shown that ERK-dependent phosphorylation of the nucleation-promoting factor WAVE2 promotes the interaction of WRC with the Arp2/3 complex and actin. This enhances Arp2/3 activation and recruitment at the leading edge [43]. Based on this evidence, we tested the hypothesis that anchoring of the AKAP2/ERK1 signaling complex to the actin cytoskeleton could favor the recruitment of the Arp2/3 complex at the leading edge of migrating cells.

To address this hypothesis, rat NVMFs were incubated with competitor or scrambled peptides and the cellular localization of the Arp2/3 complex was assessed by immunocytochemistry. As shown in Fig. 7A, a discrete pool of Arp2 localizes at the leading-edge membrane of migrating myofibroblasts incubated with the scrambled competitor peptide. In contrast, in myofibroblasts incubated with the actin competitor peptide, Arp2 was mainly detected in the cytoplasm (Fig. 7B). To quantify Arp2 recruitment at the leading edge, we measured Arp2 fluorescence intensity along an axis perpendicular to cell

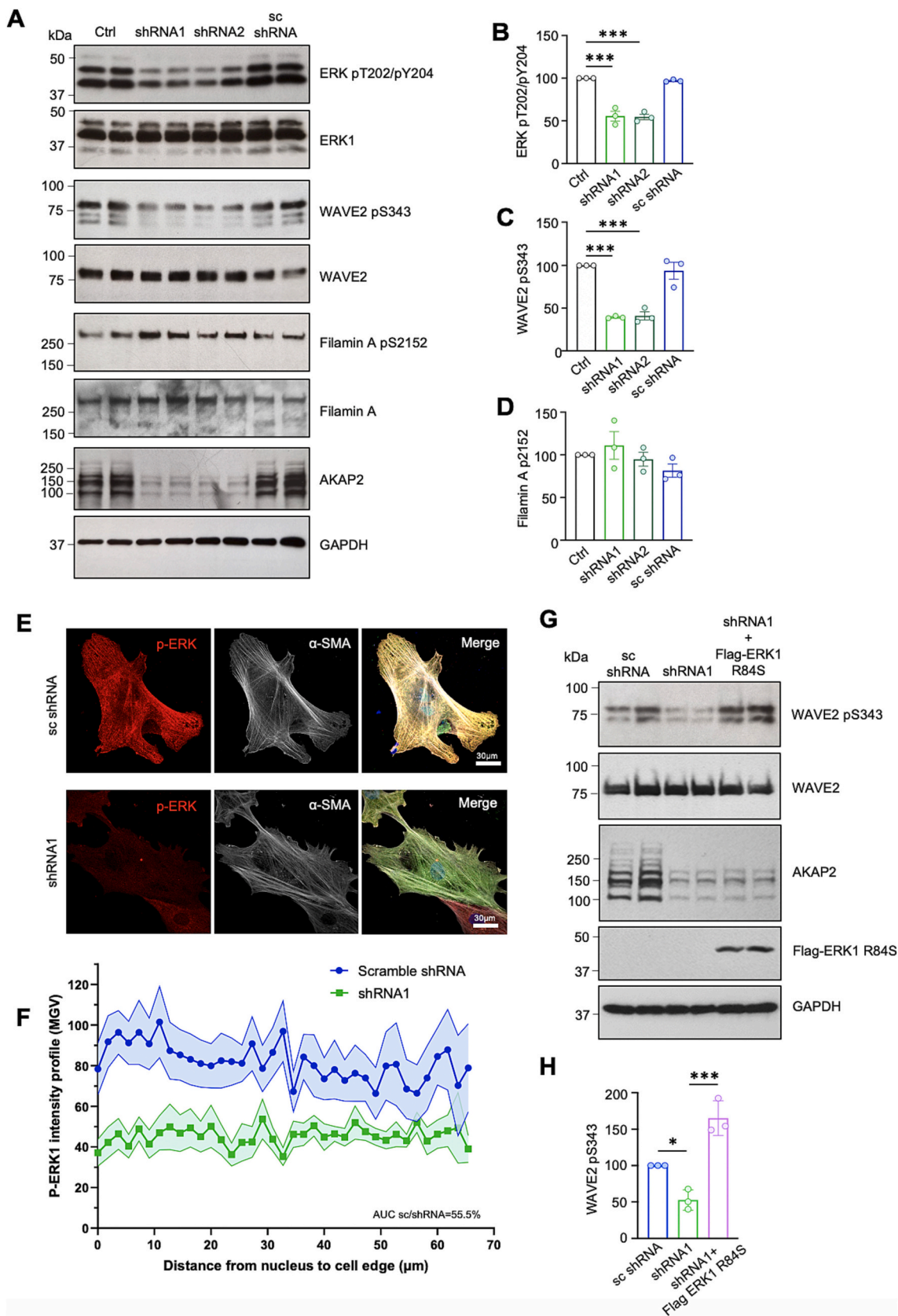
membrane. This revealed that cardiac myofibroblasts treated with the competitor peptide display a significant reduction in Arp2 levels at the leading edge compared to control cells (Fig. 7C).

To determine whether the impairment of Arp2 recruitment correlates with a reduction in the ability of cardiac myofibroblasts to migrate, we analyzed migration of individual cardiac myofibroblasts. Single-cell tracking analysis of migrating myofibroblasts incubated with the actin competitor peptide revealed a significant decrease in the total distance migrated over 72 h as compared to cells incubated with the scramble peptide (Fig. 7D–F). These findings suggest that tethering the AKAP2/ERK activation complex to F-actin favors the recruitment of the Arp2/3 complex at the lamellipodia to promote cardiac myofibroblast migration. Since cell migration is profoundly influenced by the activation state of the small molecular weight GTPases RhoA, Rac and Cdc42, we performed control experiments to determine the impact of the R<sub>11</sub>-AKAP2 319-342 disruptor peptide on the activity of the GTPases in cardiac myofibroblasts. Lysates from rat NVMFs were incubated with GST fusions of the Rho-binding domain (RBD) of Rhotekin or the Cdc42/Rac interactive binding (CRIB) motif of the p21-activated kinase to affinity precipitate GTP-bound active RhoA, Rac1 and Cdc42, respectively (Fig. S3). Results indicate that R<sub>11</sub>-AKAP2 319-342 does not affect the activity of the three GTPases suggesting that inhibitory effect of the peptide on rat NVMFs migration is not the consequence of an altered activation of RhoA, Rac1 and Cdc42 (Fig. S3).

## 4. Discussion

Cardiac myofibroblasts are the main mediators of cardiac fibrosis [6]. By invading and colonizing the myocardium of the heart subjected to stress, they contribute to excessive interstitial ECM deposition and the development of severe conduction disturbances and diastolic dysfunctions [7]. How myofibroblasts coordinate the activity of pro-migratory signaling pathways at the subcellular level to achieve effective migration in the myocardium is currently poorly understood. In this respect, in the present study we identified AKAP2 as a molecular organizer of promigratory signals at the leading edge of cardiac myofibroblasts (Fig. 8). In particular, our current data support a model where AKAP2 recruits Grb2 and ERK1 to the actin cytoskeleton to locally activate the WAVE2-Arp2/3 signaling axis, which promotes migration through the nucleation of branched actin fibers (Fig. 8). Overall, these findings indicate that AKAP2 operates as an intracellular signaling hub controlling local ERK activation to mediate efficient migration of cardiac myofibroblasts.

Our proteomic analysis of the AKAP2 interactome revealed that proteins involved in actin regulation represent the main class of AKAP2 interactors. Among these proteins one can recognize membrane receptors, adaptor proteins, kinases and Rho-guanine nucleotide exchange factor (GEFs) and transcription factors involved in pathways regulating actin polymerization, actin binding proteins, focal adhesion regulators and modulators of F-actin dynamics. These findings suggest that AKAP2 may play a central role in coordinating pro-migratory signals in cardiac



(caption on next page)

**Fig. 4.** AKAP2 mediates the phosphorylation of ERK1 and WAVE 2 in cardiac myofibroblasts. A) Rat NVMFs were infected using control lentiviruses or lentiviruses encoding wild type (AKAP2 shRNA 1 and 2) or scrambled (sc shRNA) AKAP2 shRNAs. Cell lysates were prepared 72 h after infection, loaded on SDS-PAGE gels and analyzed by Western blot. Phospho-ERK1, phospho-WAVE2 and phospho-filamin A were detected using antibodies recognizing phospho-threonine 202 and phospho-tyrosine 204 of ERK1, phospho-serine 343 of WAVE2 and phospho-serine 2152 of filamin A, respectively. The amounts of ERK1, WAVE2, Filamin A, AKAP2 and GAPDH were detected using specific antibodies, as indicated. B–D) Quantitative analysis of phosphorylated ERK1, WAVE2 and filamin A was obtained by densitometry. The amounts of phospho-ERK1, phospho-WAVE2 and phospho-filamin A were normalized to the total amounts of ERK1 (B), WAVE2 (C), filamin A (D). E) Rat NVMFs were infected using lentiviruses encoding wild type (shRNA 1) or scrambled (sc shRNA) AKAP2 shRNAs. 72 h after infection cells were stained for phospho-ERK and  $\alpha$ -SMA. F) phospho-ERK intensity was measured from the nucleus to the cell edge ( $n = 5$  cells from 3 independent experiments) and integrated by calculating the area under the curve (AUC). The mean AUC values measured in cells expressing AKAP2 shRNAs was significantly reduced (55.5 %) compared to the AUC measured in cells expressing scrambled shRNAs ( $p < 0.05$ ). G) Rat NVMFs were infected using lentiviruses encoding wild type (AKAP2 shRNA 1) or scrambled (sc shRNA) AKAP2 shRNAs and subsequently transfected with rescue a construct encoding Flag-tagged ERK1 R84S. 48 h after transfection, cell lysates were loaded on SDS-PAGE gels and analyzed by Western blot. Phospho-WAVE2, WAVE2, AKAP2 and GAPDH were detected as indicated in A). Expression of the Flag-ERK1 R84S mutant was detected using anti-Flag antibodies. H) Quantitative analysis of phosphorylated WAVE2 was obtained as indicated in B). Results presented are expressed as mean  $\pm$  S.E. of 3 independent experiments. \* $p < 0.05$ , \*\*\* $p < 0.0005$ .

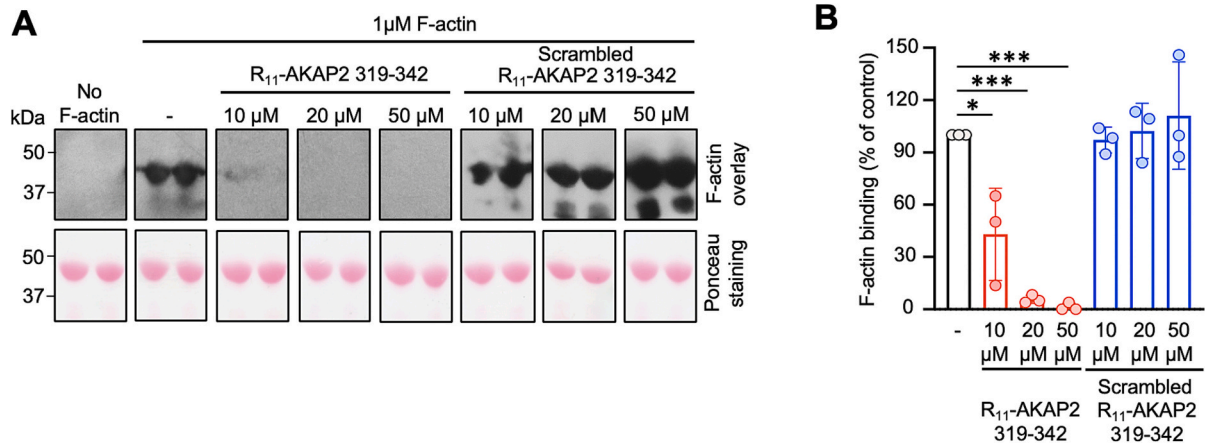


**Fig. 5.** Disruption of the AKAP2/F-actin interaction using a peptide competitor. A) The R<sub>11</sub>-AKAP2 319-342 peptide competitively inhibits the interaction between AKAP2 and F-actin. The GST-tagged AKAP2 fragment encompassing residues 331 to 491 and containing the actin-binding site was separated by SDS-PAGE and transferred onto nitrocellulose membranes. Membranes were then incubated with or without 1  $\mu$ M of F-actin in the absence or presence of the indicated concentrations of the R<sub>11</sub>-AKAP2 319-342 or the R<sub>11</sub>-AKAP2 319-342 scrambled peptides. Solid phase binding was then assessed with HRP-conjugated anti-actin antibodies. B) Quantitation of the interaction between F-actin and AKAP2. The amounts of bound F-Actin were normalized to the total protein levels (Ponceau S staining). Results are expressed as mean  $\pm$  S.E. of 3 independent experiments: \* $p < 0.05$ , \*\*\* $p < 0.0005$ .

myofibroblasts. The fact that the ERK transduction cascade emerged as the only pathway involved in actin regulation containing more than one potential AKAP2 interactor, prompted us to investigate the possible link between the AKAP2-ERK signaling axis and cardiac myofibroblast motility.

ERK1 can promote cell migration by regulating WAVE2-Arp2/3 and the RSK-filamin A transduction pathways [17,18,37,43]. The findings that AKAP2-mediated ERK activation regulates the WAVE2-Arp2/3 but not the RSK-filamin A signaling axis suggest the existence of independent and functionally segregated pools of ERK that are differentially involved in the regulation of these two pro-migratory transduction cascades. While AKAP2 might maintain ERK in proximity of WAVE2 at the leading edge of cardiac myofibroblasts, other anchoring mechanisms might direct a distinct pool of ERK at integrin-filamin A complexes, to promote RSK-mediated phosphorylation of filamin A [37], inhibition of cell adhesion and increased migration [16,37,44].

Our results that AKAP2 exerts no influence on cardiac myofibroblast proliferation (Fig. 2G) further highlight the notion that AKAP2 compartmentalizes ERK to specifically modulate pro-migratory functions in cardiac myofibroblasts. This, however, raises the question of which mechanism controls the compartmentalization of the ERK pool involved in cell proliferation. In this respect, additional AKAPs have been shown to assemble transduction units that regulate ERK. This is the case for AKAP13 (AKAP-Lbc), which associates with the MAPK scaffold KSR-1 and PKA to promote efficient ERK signaling both in the cytoplasm and in the nucleus [45,46]. Knowing that AKAP13 is expressed in cardiac myofibroblasts [23] and that nuclear ERK is a key mediator of cell

proliferation, one could raise the hypothesis of a possible implication of AKAP13 in mediating ERK-dependent proliferation of cardiac myofibroblasts. Based on the findings discussed above, it is tempting to speculate that differential targeting of ERK at separate subcellular compartments through different AKAPs may provide spatiotemporal control over migratory and proliferatory processes controlling the profibrotic activity of cardiac myofibroblasts.

Our findings indicate that AKAP2 silencing reduces phospho-ERK levels in cardiac myofibroblasts by approximately 45 % (Fig. 4). This reduction occurs both at the cell edge and intracellularly (Fig. 4) and is consistent with the fact that AKAP2 and ERK1 compartmentalize both at the leading edge of migrating cells and in intracellular compartments (Figs. 2 and 3). Based on these observations, one could raise the hypothesis that AKAP2 might anchor ERK1 at different compartments to modulate distinct cellular processes. In this respect, whereas we could show that AKAP2-anchored ERK1 controls Arp2 recruitment at the leading edge of myofibroblasts to promote migration, intracellular AKAP2-ERK1 complexes could potentially regulate additional ERK1-mediated pathways involved in functions other than migration. Future investigations will need to precisely define these additional AKAP2-mediated functions.

We have previously shown that AKAP13 modulates cardiac myofibroblast motility through the activation of the small molecular weight GTPase RhoA [23]. By acting as a RhoA-activating GEF, AKAP13 favors the formation of RhoA-GTP, which, in turn, regulates actin polymerization and myofibroblast motility [47]. Our current findings that AKAP2 maintains an F-actin-bound ERK-dependent promigratory signaling

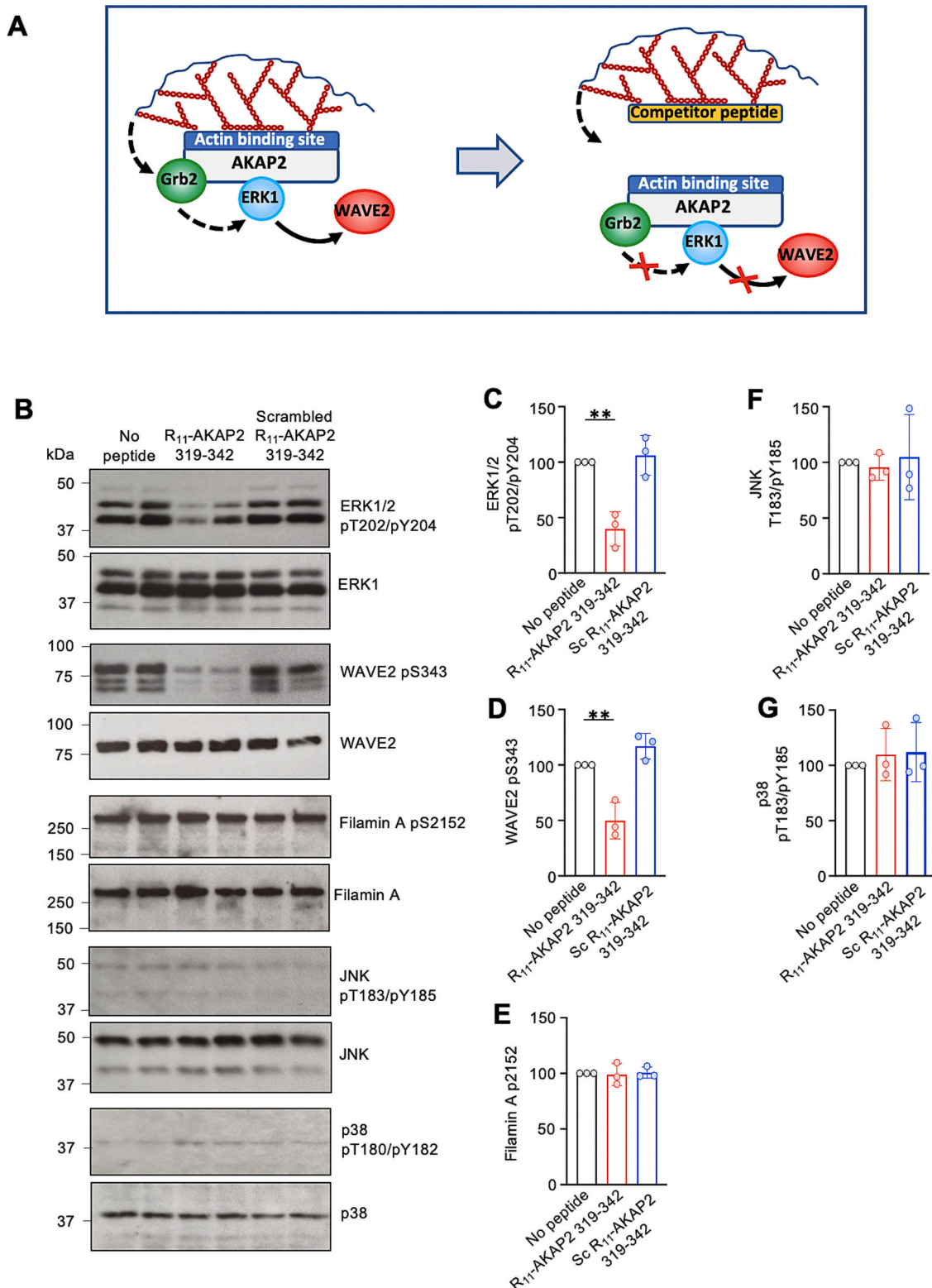


**Fig. 6.** AKAP2 interaction with F-actin promotes ERK1-mediated activation of WAVE 2. A) Schematic representation of the proposed signaling pathway where AKAP2 scaffolds GRB2 and ERK1 proteins to the actin cytoskeleton to promote WAVE2 phosphorylation and activation (upper panel). By binding to F-actin, the cell permeant competitor peptide R<sub>11</sub>-AKAP2 319-342 disrupts the interaction between AKAP2 and the actin cytoskeleton resulting in the inhibition of ERK1 and WAVE2 signaling. B) Rat NVMFs were incubated with 20 μM of either R<sub>11</sub>-AKAP2 319-342 or scrambled R<sub>11</sub>-AKAP2 319-342 for 1 h. Cell lysates were then loaded on SDS-PAGE gels and analyzed by Western blot. Phospho-ERK1, phospho-WAVE2, phospho-Filamin A were detected as indicated in Fig. 4. Phospho-JNK and phospho p38 were detected using antibodies recognizing phospho-threonine 183 and phospho-tyrosine 185 of JNK, and phospho-threonine 180 and phospho-tyrosine 182 of p38, respectively. The amounts of ERK1, WAVE2, filamin A, JNK and p38 were detected using specific antibodies, as indicated. C–G) Quantitative analysis of phosphorylated ERK1, WAVE2, filamin A, JNK and p38 was obtained by densitometry. The amounts of phospho-ERK1, phospho-WAVE2 and phospho-filamin A, phospho-JNK and phospho-p38 were normalized to the total amounts of ERK1 (C), WAVE2 (D), filamin A (E), JNK (F) and p38 (G). Results presented are expressed as mean ± S.E. of 3 independent experiments: \*\**p* < 0.005.

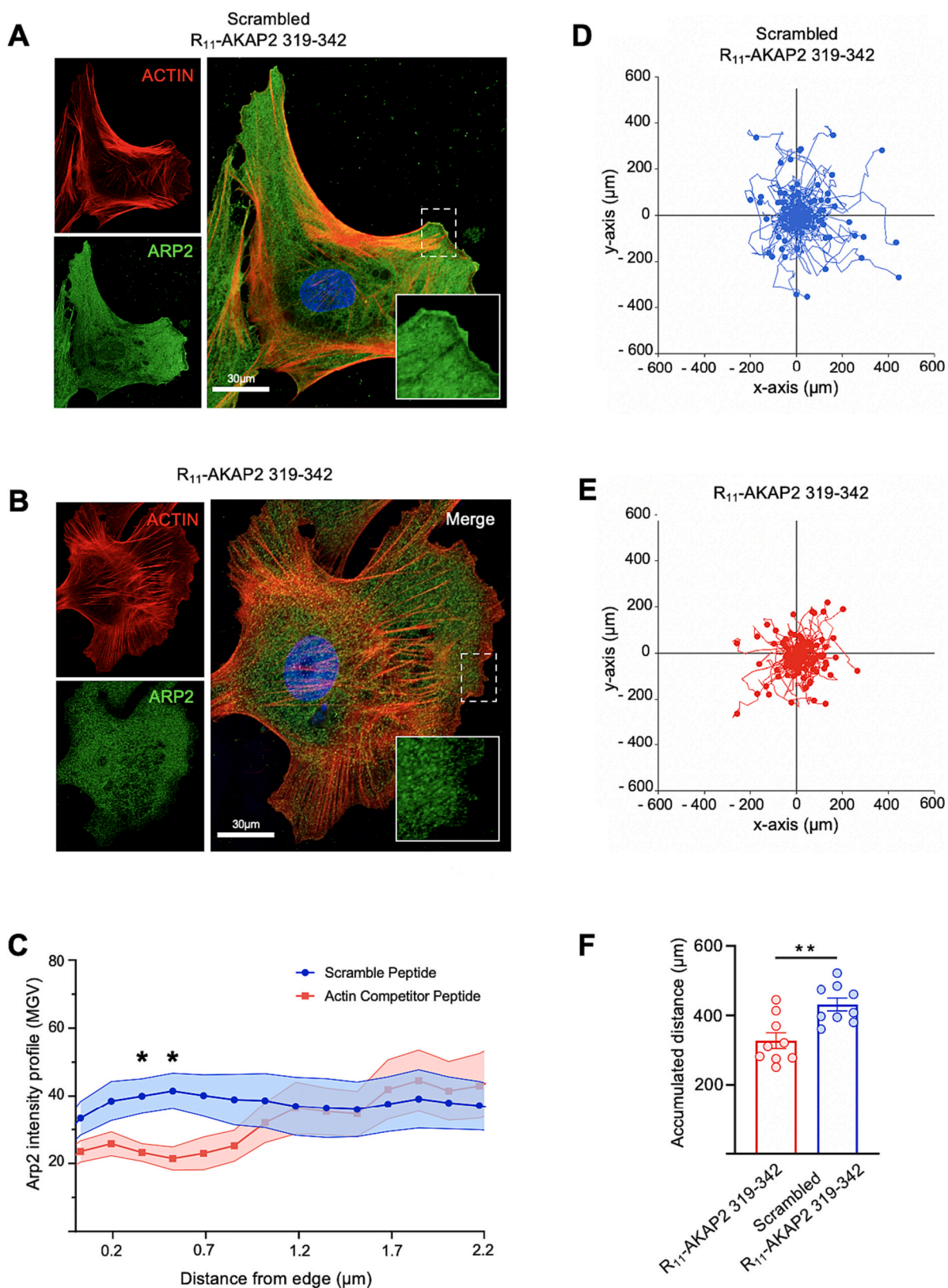


**Fig. 7.** AKAP2 interaction with F-actin mediates ARP2 localization at the leading edge of migrating cells. **A, B)** Rat NVMFs were incubated for 8 h with 20 μM of R<sub>11</sub>-AKAP2 319-342 or scrambled R<sub>11</sub>-AKAP2 319-342 and stained for Arp2 and the actin cytoskeleton. **C)** Arp2 intensity was measured over a distance of 2 μm from the cell edge (n = 10 cells from 3 independent experiments). \*p < 0.05 as compared to rat NVMFs incubated with the scrambled R<sub>11</sub>-AKAP2 319-342 peptide. **D–E)** Random migration of rat NVMFs incubated with 20 μM of R<sub>11</sub>-AKAP2 319-342 (**D**) or scrambled R<sub>11</sub>-AKAP2 319-342 (**E**) was imaged using time-lapse microscopy for 8 h. Migration trajectories were determined on a total of 90 cells from 3 independent experiments. **F)** Average migration trajectory lengths expressed in μm calculated for rat NVMFs incubated with 20 μM either R<sub>11</sub>-AKAP2 319-342 or Scrambled R<sub>11</sub>-AKAP2 319-342. Results are expressed as mean ± SE of 9 independent experiments: \*\*p < 0.005.

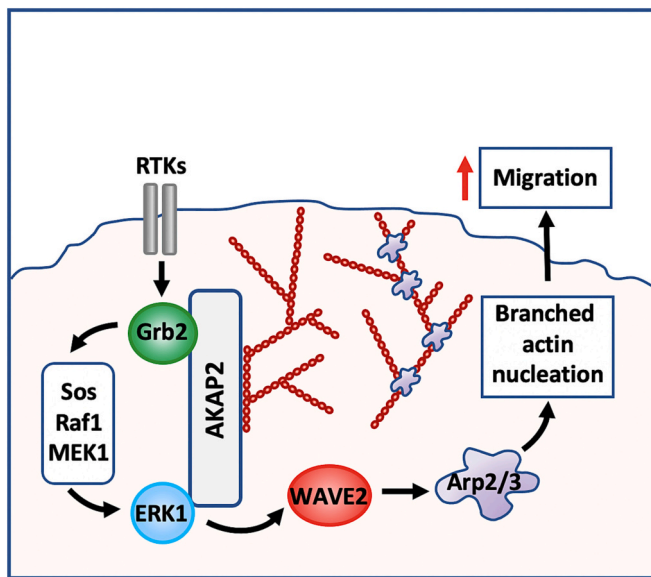


**Fig. 8.** Model illustrating the role of AKAP2 in directing ERK1 dependent activation of WAVE 2 and ARP2. Upon extracellular cues that drives tyrosine kinase receptor (TKR) activation, GRB2 scaffolded by AKAP2 induces the activation of Sos and the downstream MAPK signaling pathway leading to ERK1 activation. Active ERK1 induces the phosphorylation of WAVE2, which, in turn, promotes the recruitment of the Arp2/3 actin nucleation complex at the leading edge. This contributes to actin nucleation and polymerization at the leading edge, thereby promoting cell migration.

complex that localizes at the leading edge suggest that AKAPs can organize transduction cascades that regulate multiple aspects of the migratory process. Indeed, while Arp2/3 regulation by AKAP2 at the cell leading edge is expected to promote the nucleation of branched actin filaments that control lamellipodia protrusion [15], RhoA regulation by AKAP13 might impact the formation of stress fibers which play a key role in tail retraction during migration [48]. Interestingly, AKAP13 has also been shown to contribute to the generation of PKA activity gradients at the cell leading edge [49]. While the implication of these findings has not been investigated directly in cardiac myofibroblasts, targeting PKA at the leading edge by AKAP13 might potentially contribute to lamellipodia dynamics [50].

Recent findings obtained in our laboratory indicate that AKAP2 is overexpressed in prostatic neuroendocrine carcinoma (PNEC), a highly metastatic subtype of prostate cancer [51], where it controls cancer cell migration and invasion [38]. In these cells, AKAP2 anchors protein phosphatase 1 (PP1) to the actin cytoskeleton to favor dephosphorylation and activation of the actin severing protein cofilin, thus enhancing F-actin dynamics and promoting migration [38]. This suggests that the mechanisms whereby AKAP2 regulates cell migration are cell type-dependent. Whereas the ability of AKAP2 to promote PNEC cell migration rely on the anchoring of a phosphatase and the modulation of actin turnover, the effects of the anchoring protein on cardiac myofibroblast motility proceed through the assembly of an ERK activation complex that promotes branched actin polymerization. Therefore, it appears that AKAP2 functions as a versatile anchoring protein that assembles cell type-specific promigratory signaling complexes containing different repertoires of signaling enzymes. It is currently unknown which regulatory process allows AKAP2 to differentially recruit transduction molecules. Possible mechanisms might include cell type-specific post-translational modifications that impact the affinity of the interactions between AKAP2 and its binding partners, or, more simply, cell type-specific genomic programs that differentially impact the expression of AKAP2-anchored enzymes.

In the current study, we developed cell-permeant peptides that successfully disrupted the interaction between AKAP2 and F-actin and that

significantly reduced the ability of AKAP2 to activate the promigratory ERK-WAVE-Arp2/3 signaling pathway. These results suggest that recruitment of the AKAP2-dependent ERK activation complex at the actin cytoskeleton is necessary to locally activate the kinase and its downstream effectors. In this respect, one could speculate that AKAP2 might localize ERK and Grb2 in proximity of tyrosine kinase receptors clustered at the leading edge of migrating cells [52]. In this configuration, activating signals originating from the receptors would be transmitted to AKAP2-anchored ERK and then sequentially to WAVE2 and Arp2/3.

The competitor peptide developed in this study is based upon the sequence of the F-actin binding site on AKAP2 [38]. The fact that this sequence is not conserved in other actin-binding proteins reduces the possibility of interference with other protein-actin interactions in cardiac myofibroblasts [38]. In this respect, future experiments will need to evaluate whether intracardiac injection of cell-permeant peptides inhibiting the AKAP2-F-actin interaction could represent a valuable approach to selectively target AKAP2/F-actin complexes in cardiac myofibroblasts, and, consequently, to reduce myocardial fibrosis.

## 5. Conclusions

In conclusion, our current findings have several implications. Firstly, they provide evidence that AKAP2 localizes at the leading edge of migrating cardiac myofibroblasts where it interacts with actin. Secondly, they suggest that the AKAP2 forms an ERK activation complex involved in the activation of an ERK-dependent promigratory pathway that leads to the translocation of Arp2 at the leading edge membrane. Thirdly, they indicate that cell permeant peptides disrupting the interaction between AKAP2 and F-actin can be used to inhibit Arp2 translocation and cardiac myofibroblast migration. This suggests that AKAP2 is an F-actin bound scaffold controlling the local processing of promigratory signals in cardiac myofibroblasts.

## Ethical approval and consent to participate

All animal experiments were performed according to the guideline for care and use of laboratory animals and approved by the Swiss Government Veterinary Office (authorization VD3680 and VD3681).

## CRediT authorship contribution statement

**Marion Delaunay:** Conceptualization, Data curation, Formal analysis, Investigation, Methodology, Writing – original draft. **Aleksandra Paterek:** Data curation, Formal analysis, Methodology, Investigation. **Ivan Gautschi:** Methodology. **Greta Scherler:** Investigation, Methodology. **Dario Diviani:** Conceptualization, Formal analysis, Funding acquisition, Investigation, Supervision, Writing – review & editing.

## Declaration of competing interest

The authors declare that they have no known competing financial interests or personal relationships that could have appeared to influence the work reported in this paper.

## Data availability

Data will be made available on request.

## Acknowledgments

We are grateful to Simon Kaiser for critically reviewing the manuscript. This work was supported by grants 31003A\_175838 and 310030\_212245 of the Swiss National Science Foundation (to D.D).

## Appendix A. Supplementary data

Supplementary data to this article can be found online at <https://doi.org/10.1016/j.bbamcr.2024.119674>.

## References

- [1] J.A. Towbin, N.E. Bowles, The failing heart, *Nature* 415 (6868) (2002) 227–233.
- [2] J.A. Hill, E.N. Olson, Cardiac plasticity, *New Engl. J. Med.* 358 (13) (2008) 1370–1380.
- [3] H. Sadek, E.N. Olson, Toward the goal of human heart regeneration, *Cell Stem Cell* 26 (1) (2020) 7–16.
- [4] M. Xin, E.N. Olson, R. Bassel-Duby, Mending broken hearts: cardiac development as a basis for adult heart regeneration and repair, *Nat. Rev. Mol. Cell Biol.* 14 (8) (2013) 529–541.
- [5] J.S. Burchfield, M. Xie, J.A. Hill, Pathological ventricular remodeling: mechanisms: part 1 of 2, *Circulation* 128 (4) (2013) 388–400.
- [6] N.G. Frangogiannis, Cardiac fibrosis, *Cardiovasc. Res.* 117 (6) (2021) 1450–1488.
- [7] M. Amoni, E. Dries, S. Ingelaere, D. Vermoortele, H.L. Roderick, P. Claus, R. Willems, K.R. Sipido, Ventricular arrhythmias in ischemic cardiomyopathy—new avenues for mechanism-guided treatment, *Cells* 10 (10) (2021).
- [8] C.A. Souders, S.L. Bowers, T.A. Baudino, Cardiac fibroblast: the renaissance cell, *Circ. Res.* 105 (12) (2009) 1164–1176.
- [9] J.G. Travers, F.A. Kamal, J. Robbins, K.E. Yutzey, B.C. Blaxall, Cardiac fibrosis: the fibroblast awakens, *Circ. Res.* 118 (6) (2016) 1021–1040.
- [10] H. Khalil, O. Kanisicak, V. Prasad, R.N. Correll, X. Fu, T. Schips, R.J. Vagnozzi, R. Liu, T. Huynh, S.J. Lee, J. Karch, J.D. Molkenkin, Fibroblast-specific TGF-beta-Smad2/3 signaling underlies cardiac fibrosis, *J. Clin. Invest.* 127 (10) (2017) 3770–3783.
- [11] M.D. Tallquist, J.D. Molkenkin, Redefining the identity of cardiac fibroblasts, *Nat. Rev. Cardiol.* 14 (8) (2017) 484–491.
- [12] K. Rottner, J. Faix, S. Bogdan, S. Linder, E. Kerkhoff, Actin assembly mechanisms at a glance, *J. Cell Sci.* 130 (20) (2017) 3427–3435.
- [13] P. Bieling, K. Rottner, From WRC to Arp2/3: collective molecular mechanisms of branched actin network assembly, *Curr. Opin. Cell Biol.* 80 (2023) 102156.
- [14] D. Brandt, M. Gimona, M. Hillmann, H. Haller, H. Mischak, Protein kinase C induces actin reorganization via a Src- and Rho-dependent pathway, *J. Biol. Chem.* 277 (23) (2002) 20903–20910.
- [15] S.H. Soderling, Grab your partner with both hands: cytoskeletal remodeling by Arp2/3 signaling, *Sci. Signal.* 2 (55) (2009) pe5.
- [16] H. Lavoie, J. Gagnon, M. Therrien, ERK signalling: a master regulator of cell behaviour, life and fate, *Nat. Rev. Mol. Cell Biol.* 21 (10) (2020) 607–632.
- [17] M.C. Mendoza, E.E. Er, W. Zhang, B.A. Ballif, H.L. Elliott, G. Danuser, J. Blenis, ERK-MAPK drives lamellipodia protrusion by activating the WAVE2 regulatory complex, *Mol. Cell* 41 (6) (2011) 661–671.
- [18] M.C. Mendoza, M. Vilela, J.E. Juarez, J. Blenis, G. Danuser, ERK reinforces actin polymerization to power persistent edge protrusion during motility, *Sci. Signal.* 8 (377) (2015) ra47.
- [19] J.D. Scott, C.W. Dessauer, K. Tasken, Creating order from chaos: cellular regulation by kinase anchoring, *Annu. Rev. Pharmacol. Toxicol.* 53 (2013) 187–210.
- [20] M. Delaunay, H. Osman, S. Kaiser, D. Diviani, The role of cyclic AMP signaling in cardiac fibrosis, *Cells* 9 (1) (2019).
- [21] P.J. Bucko, J.D. Scott, Drugs that regulate local cell signaling: AKAP targeting as a therapeutic option, *Annu. Rev. Pharmacol. Toxicol.* 61 (2021) 361–379.
- [22] M.H. Omar, J.D. Scott, AKAP signaling islands: venues for precision pharmacology, *Trends Pharmacol. Sci.* 41 (12) (2020) 933–946.
- [23] S. Cavin, D. Maric, D. Diviani, A-kinase anchoring protein-Lbc promotes profibrotic signaling in cardiac fibroblasts, *Biochim. Biophys. Acta* 1843 (2) (2014) 335–345.
- [24] C.D. del Vecovo, S. Cotecchia, D. Diviani, A-kinase-anchoring protein-Lbc anchors IkkappaB kinase beta to support interleukin-6-mediated cardiomyocyte hypertrophy, *Mol. Cell Biol.* 33 (1) (2013) 14–27.
- [25] D. Maric, A. Paterek, M. Delaunay, I.P. Lopez, M. Arambasic, D. Diviani, A-kinase anchoring protein 2 promotes protection against myocardial infarction, *Cells* 10 (11) (2021).
- [26] J.J. Santiago, A.L. Dangerfield, S.G. Rattan, K.L. Bathe, R.H. Cunningham, J. E. Raizman, K.M. Bedosky, D.H. Freed, E. Kardami, I.M. Dixon, Cardiac fibroblast to myofibroblast differentiation in vivo and in vitro: expression of focal adhesion components in neonatal and adult rat ventricular myofibroblasts, *Dev. Dyn.* 239 (6) (2010) 1573–1584.
- [27] M. Wilm, A. Shevchenko, T. Houthaeve, S. Breit, L. Schweigerer, T. Fotsis, M. Mann, Femtomole sequencing of proteins from polyacrylamide gels by nano-electrospray mass spectrometry, *Nature* 379 (6564) (1996) 466–469.
- [28] F. Meier, A.D. Brunner, S. Koch, H. Koch, M. Lubeck, M. Krause, N. Goedecke, J. Decker, T. Kosinski, M.A. Park, N. Bache, O. Hoerning, J. Cox, O. Rother, M. Mann, Online parallel accumulation-serial fragmentation (PASEF) with a novel trapped ion mobility mass spectrometer, *Mol. Cell. Proteomics* 17 (12) (2018) 2534–2545.
- [29] J. Cox, M. Mann, MaxQuant enables high peptide identification rates, individualized p.p.b.-range mass accuracies and proteome-wide protein quantification, *Nat. Biotechnol.* 26 (12) (2008) 1367–1372.
- [30] J. Cox, N. Neuhauser, A. Michalski, R.A. Scheltema, J.V. Olsen, M. Mann, Andromeda: a peptide search engine integrated into the MaxQuant environment, *J. Proteome Res.* 10 (4) (2011) 1794–1805.
- [31] B. Schwannhauser, D. Busse, N. Li, G. Dittmar, J. Schuchhardt, J. Wolf, W. Chen, M. Selbach, Corrigendum: global quantification of mammalian gene expression control, *Nature* 495 (7439) (2013) 126–127.
- [32] S. Tyanova, T. Temu, P. Sinitcyn, A. Carlson, M.Y. Hein, T. Geiger, M. Mann, J. Cox, The Perseus computational platform for comprehensive analysis of (prote) omics data, *Nat. Methods* 13 (9) (2016) 731–740.
- [33] J. Cox, M. Mann, 1D and 2D annotation enrichment: a statistical method integrating quantitative proteomics with complementary high-throughput data, *BMC Bioinformatics* 13 (Suppl. 16) (2012) S12.
- [34] Y. Perez-Riverol, J. Bai, C. Bandla, D. Garcia-Seisdedos, S. Hewapathirana, S. Kamatchinathan, D.J. Kundu, A. Prakash, A. Frericks-Zipper, M. Eisenacher, M. Walzer, S. Wang, A. Brazma, J.A. Vizcaino, The PRIDE database resources in 2022: a hub for mass spectrometry-based proteomics evidences, *Nucleic Acids Res.* 50 (D1) (2022) D543–D552.
- [35] W. da Huang, B.T. Sherman, R.A. Lempicki, Systematic and integrative analysis of large gene lists using DAVID bioinformatics resources, *Nat. Protoc.* 4 (1) (2009) 44–57.
- [36] C. Huang, K. Jacobson, M.D. Schaller, MAP kinases and cell migration, *J. Cell Sci.* 117 (Pt 20) (2004) 4619–4628.
- [37] M.S. Woo, Y. Ohta, I. Rabinovitz, T.P. Stossel, J. Blenis, Ribosomal S6 kinase (RSK) regulates phosphorylation of filamin A on an important regulatory site, *Mol. Cell Biol.* 24 (7) (2004) 3025–3035.
- [38] E. Reggi, S. Kaiser, N. Sahnane, S. Uccella, S. La Rosa, D. Diviani, AKAP2-anchored protein phosphatase 1 controls prostatic neuroendocrine carcinoma cell migration and invasion, *Biochim. Biophys. Acta Mol. basis Dis.* 1870 (1) (2024) 166916.
- [39] M.G. Gold, B. Lygren, P. Dokurno, N. Hoshi, G. McConnachie, K. Tasken, C. R. Carlson, J.D. Scott, D. Barford, Molecular basis of AKAP specificity for PKA regulatory subunits, *Mol. Cell* 24 (3) (2006) 383–395.
- [40] C.R. Carlson, B. Lygren, T. Berge, N. Hoshi, W. Wong, K. Tasken, J.D. Scott, Delineation of type I protein kinase A-selective signaling events using an RI anchoring disruptor, *J. Biol. Chem.* 281 (30) (2006) 21535–21545.
- [41] A. Dema, E. Perets, M.S. Schulz, V.A. Deak, E. Klussmann, Pharmacological targeting of AKAP-directed compartmentalized cAMP signalling, *Cell. Signal.* 27 (12) (2015) 2474–2487.
- [42] K.G. Campellone, M.D. Welch, A nucleator arms race: cellular control of actin assembly, *Nat. Rev. Mol. Cell Biol.* 11 (4) (2010) 237–251.
- [43] C.M. Danson, S.M. Pocha, G.B. Bloomberg, G.O. Cory, Phosphorylation of WAVE2 by MAP kinases regulates persistent cell migration and polarity, *J. Cell Sci.* 120 (Pt 23) (2007) 4144–4154.
- [44] I. Lamsoul, L. Dupre, P.G. Lutz, Molecular tuning of filamin A activities in the context of adhesion and migration, *Front. Cell Dev. Biol.* 8 (2020) 591323.
- [45] F.D. Smith, L.K. Langeberg, C. Cellurale, T. Pawson, D.K. Morrison, R.J. Davis, J. D. Scott, AKAP-Lbc enhances cyclic AMP control of the ERK1/2 cascade, *Nat. Cell Biol.* 12 (12) (2010) 1242–1249.
- [46] F.D. Smith, L.K. Langeberg, J.D. Scott, Plugging PKA into ERK scaffolds, *Cell Cycle* 10 (5) (2011) 731–732.
- [47] D. Diviani, J. Soderling, J.D. Scott, AKAP-Lbc anchors protein kinase A and nucleates Galpha 12-selective Rho-mediated stress fiber formation, *J. Biol. Chem.* 276 (47) (2001) 44247–44257.
- [48] S. Pellegrin, H. Mellor, Actin stress fibres, *J. Cell Sci.* 120 (Pt 20) (2007) 3491–3499.
- [49] A.A. Paulucci-Holthausen, L.A. Vergara, L.J. Bellot, D. Canton, J.D. Scott, K. L. O'Connor, Spatial distribution of protein kinase A activity during cell migration is mediated by A-kinase anchoring protein AKAP Lbc, *J. Biol. Chem.* 284 (9) (2009) 5956–5967.
- [50] D. Zhang, J. Ouyang, N. Wang, Y. Zhang, J. Bie, Y. Zhang, Promotion of PDGF-induced endothelial cell migration by phosphorylated VASP depends on PKA anchoring via AKAP, *Mol. Cell. Biochem.* 335 (1–2) (2010) 1–11.
- [51] L. Puca, P.J. Vlachostergios, H. Beltran, Neuroendocrine differentiation in prostate cancer: emerging biology, models, and therapies, *Cold Spring Harb. Perspect. Med.* 9 (2) (2019).
- [52] G.K. Chan, J.A. McGrath, M. Parsons, Spatial activation of ezrin by epidermal growth factor receptor and focal adhesion kinase co-ordinates epithelial cell migration, *Open Biol.* 11 (8) (2021) 210166.